

**Land Cover/Land Use Changes (LC/LUC) and Impacts on Environment
in South/Southeast Asia - International Regional Science Meeting
28-30th May, 2018, Philippines**

Atmospheric Aerosols and Their Influence on Urban Air Quality in Malaysia

Arnis Asmat

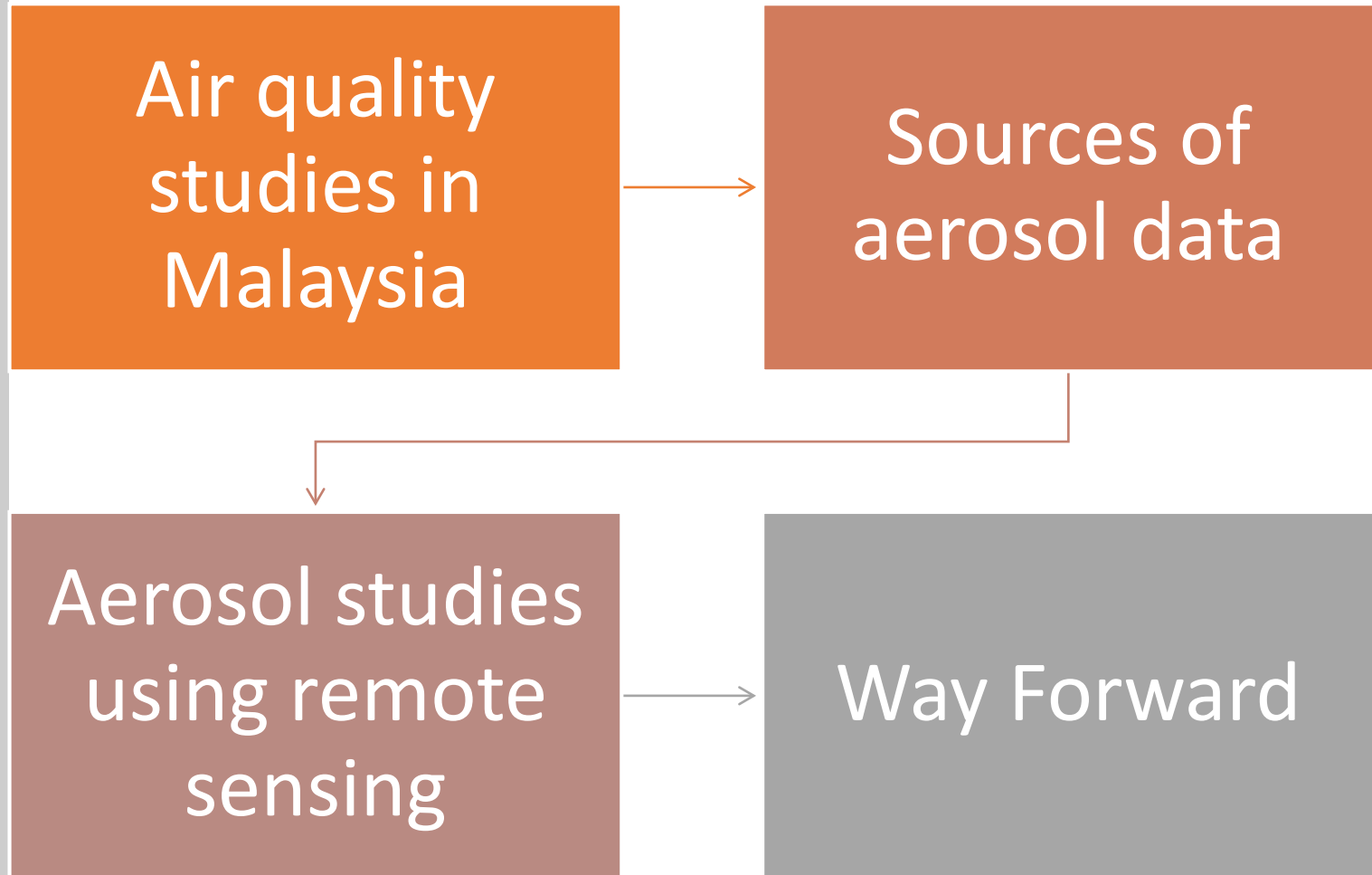
School Of Chemistry & Environmental Studies

University Teknologi MARA (UiTM)

Shah Alam, Selangor

MALAYSIA

OUTLINE



Air Quality Studies in Malaysia

- Air pollution -serious environmental problem in the developing Southeast Asian countries
- Major sources of air pollution – urbanisation & associated industrial and transportation activities, land clearing, open burning & forest fire.
- Trans-boundary aerosols transport –southwest monsoon
- Effects:
 - Health
 - Poor visibility
 - Radiative forcing
- Aerosols large uncertainties in earth's climate system due to their high spatio-temporal variability and various optical properties
- Radiative it's absorb and scatter the radiation through the atmosphere depending on their chemical and physical characteristics and also can indirectly change the cloud condensation nuclei [Oh et al. 2004].
- Changes in aerosol loadings, composition of aerosols and aerosols size distribution will lead to the differences in aerosol optical properties [Rozwadowska et al. 2010].

History

Haze History in Malaysia

YEAR	HIGHEST API VALUE (VENUE)	NOTES
1983	API Data not available	<ul style="list-style-type: none">• First record of haze in Malaysia
1997	839 (Kuching)	<ul style="list-style-type: none">• Worsened by El Nino• Haze emergency declared in Sarawak• Caused by forest and peat fires• 29 Continuous Air Quality Monitoring Stations (CAQMS) had PM10 concentration exceeding the Malaysian Ambient Air Quality Guidelines (MAAQQ)
2005	541 (Kuala Selangor)	<ul style="list-style-type: none">• Haze emergency was declared in 11 August• Few flights were suspended

(ASM, 2016)

History

Haze History in Malaysia

YEAR	HIGHEST API VALUE (VENUE)	NOTES
2006	222 (Sri Aman)	<ul style="list-style-type: none">• Moderate haze episodes in mid-July, mid-August and late September to October 2006• 20 stations in Peninsular Malaysia recorded API value 101-200
2009	299 (Sibu)	<ul style="list-style-type: none">• Haze began in early June 2009 and progressively became worse toward July• Primary cause of this event was the slash and burn practices used to clear land for agricultural purposes in Sumatra, Indonesia
2010	432 (Muar)	<ul style="list-style-type: none">• Due to transboundary haze as a result of land and forest fires from Central Sumatera• Short period of haze episode from 19-23 October• Occurred in southern part of Peninsular Malaysia• Schools were closed in Muar on 21 October

(ASM, 2016)

History

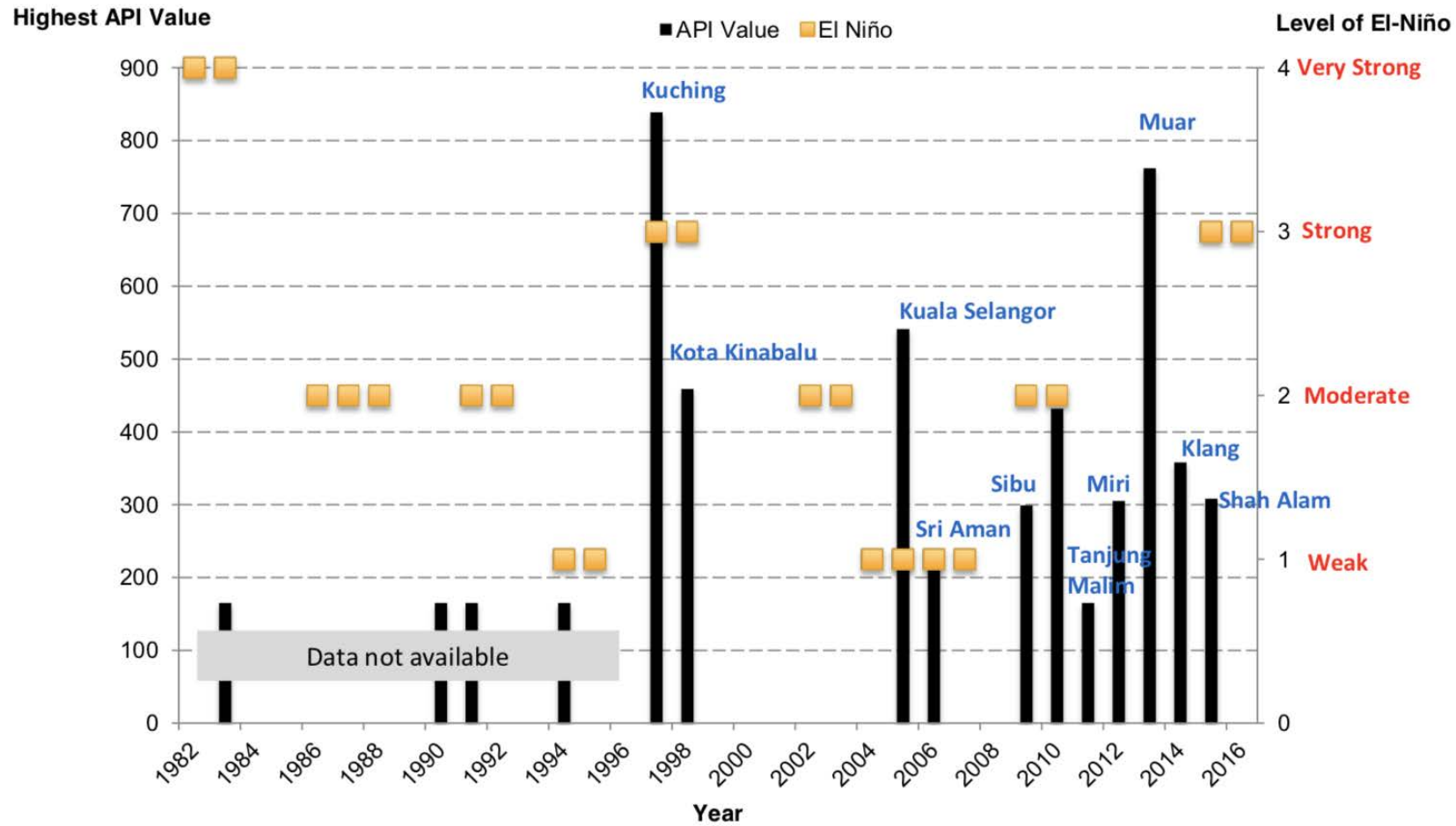
Haze History in Malaysia

YEAR	HIGHEST API VALUE (VENUE)	NOTES
2013	762 (Muar)	<ul style="list-style-type: none">• Short period of severe haze episode from 15 to 27 June 2013 due to transboundary pollution• The most affected areas were Johor, Melaka and Negeri Sembilan• <u>Haze Emergency</u> was declared on 23 June 2013 in Muar and Ledang Districts, Johor. The Haze Emergency was lifted on 24 June 2013
2015	308 (Shah Alam)	<ul style="list-style-type: none">• Deterioration of air quality from August to September due to massive land and forest fires in Sumatra and Kalimantan• Considered as the worst after 1997 Haze due to prolonged haze duration (>2 months)

(ASM, 2016)

History

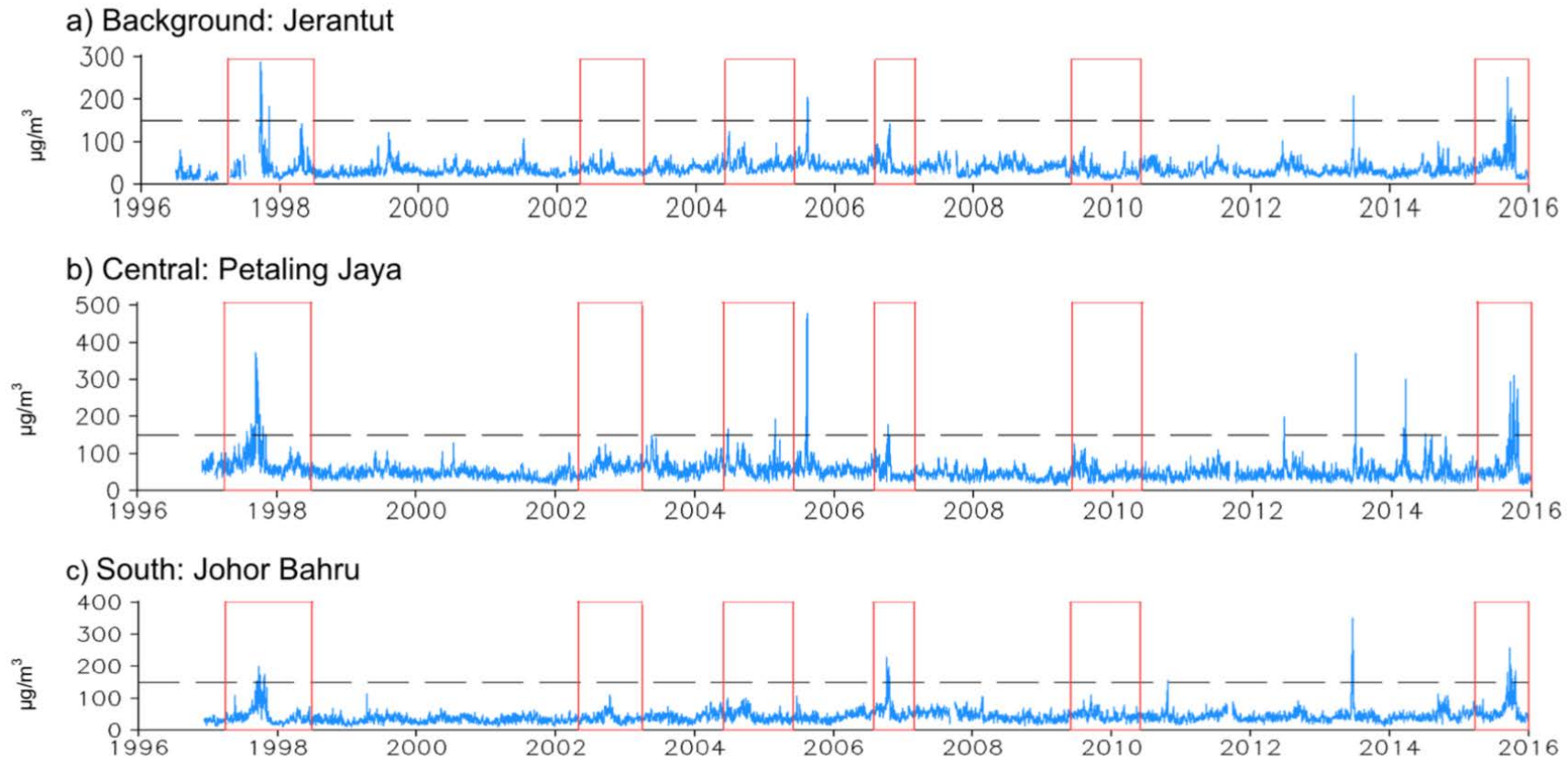
Haze History in Malaysia



Note: All of this API is based on PM₁₀

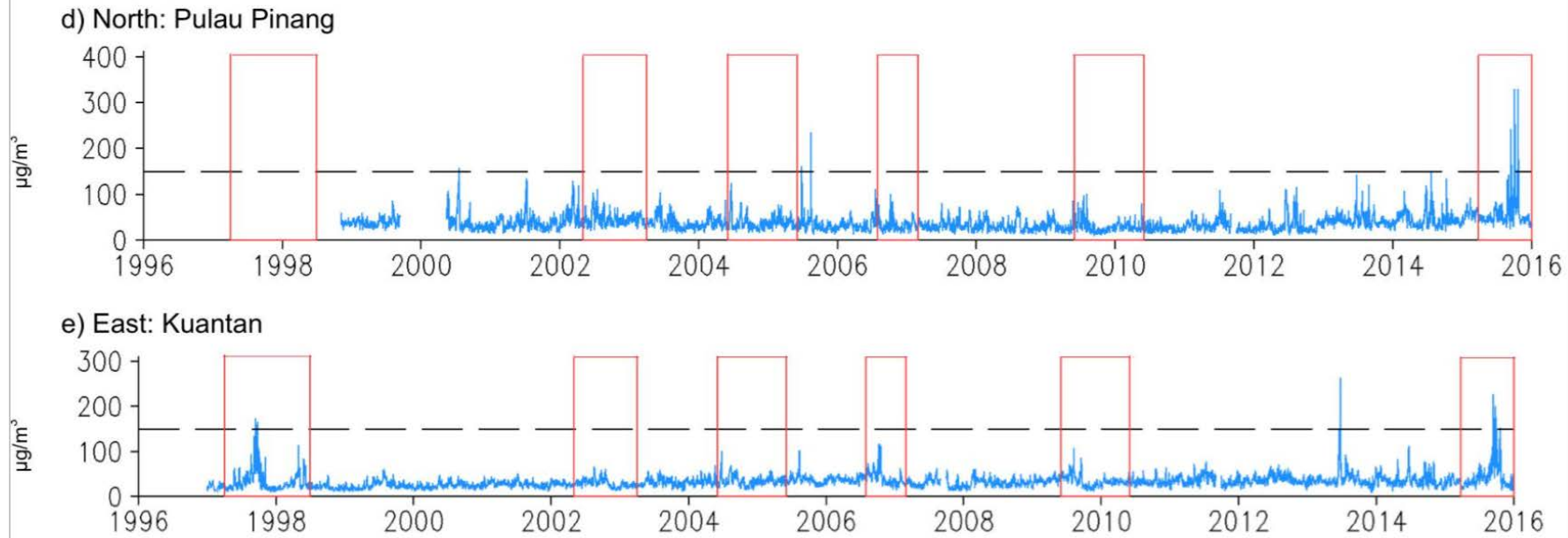
Trends of PM10 daily mean concentration (1996-2015)

Trends of Particulate Matter



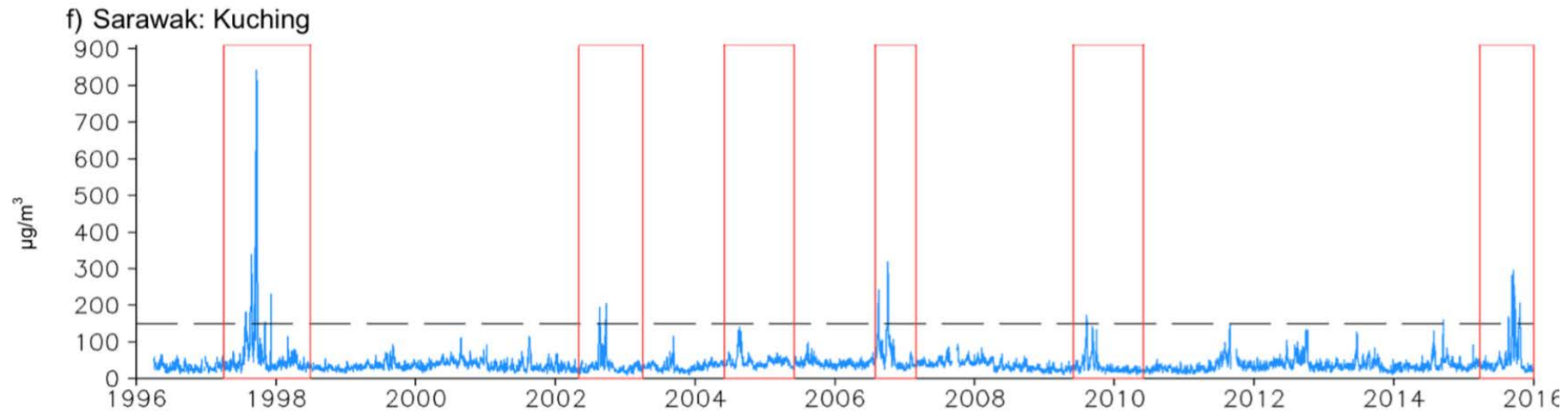
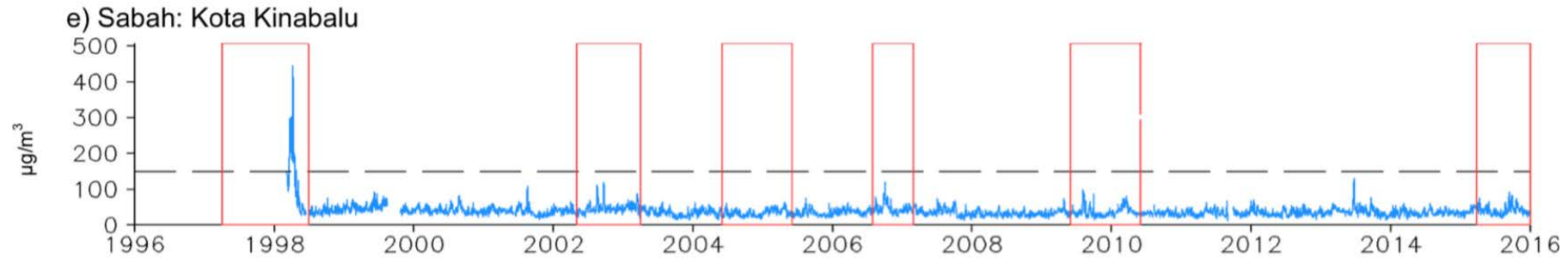
Trends of PM10 daily mean concentration (1996-2015)

Trends of Particulate Matter



Trends of PM10 daily mean concentration (1996-2015)

Trends of Particulate Matter



Source of Haze Based on Satellite Image



a) Satellite image during haze episode in 2001 (NASA 2016)

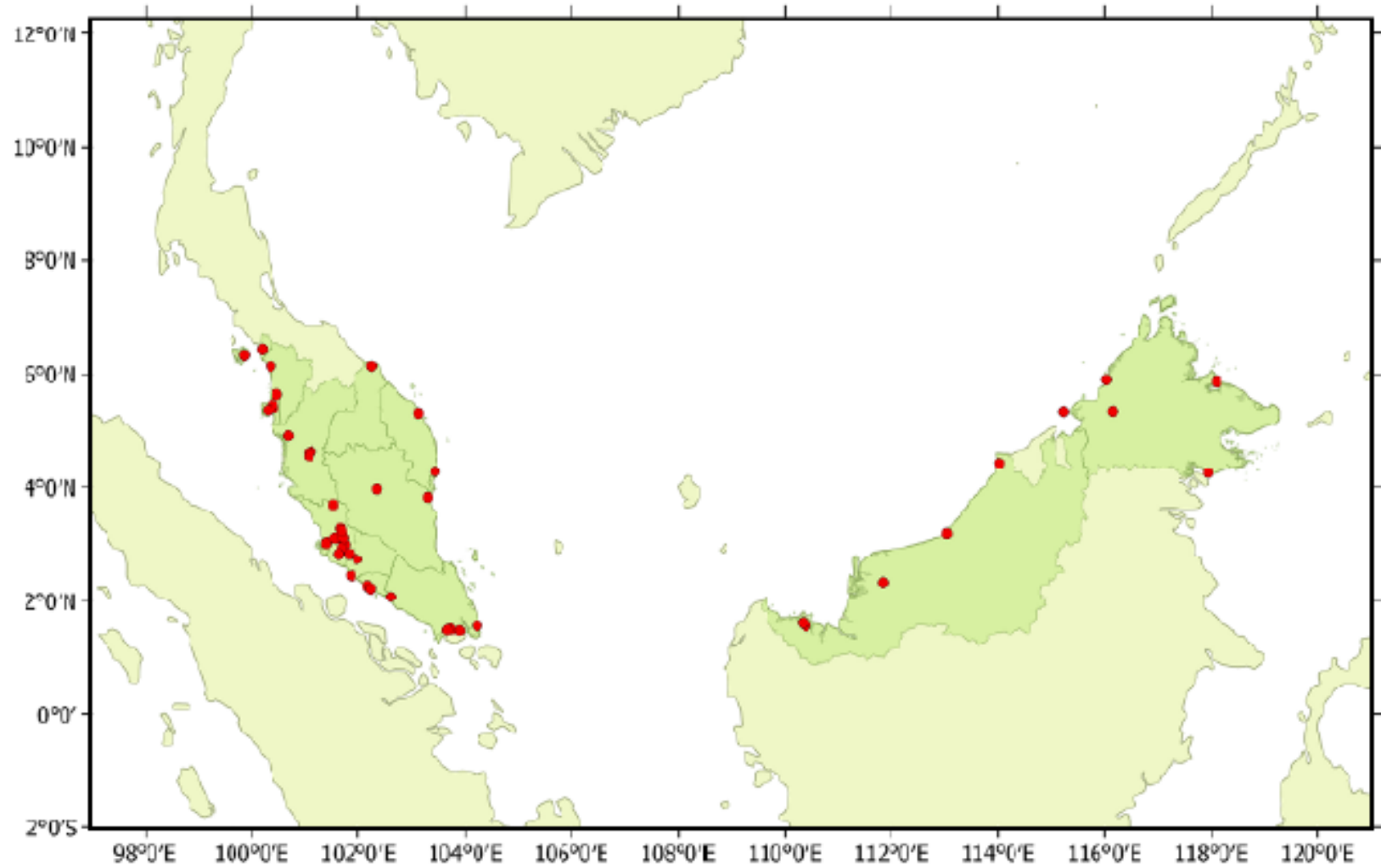


b) Haze episode in September 2015 (NASA 2015)

Air Quality Monitoring Network

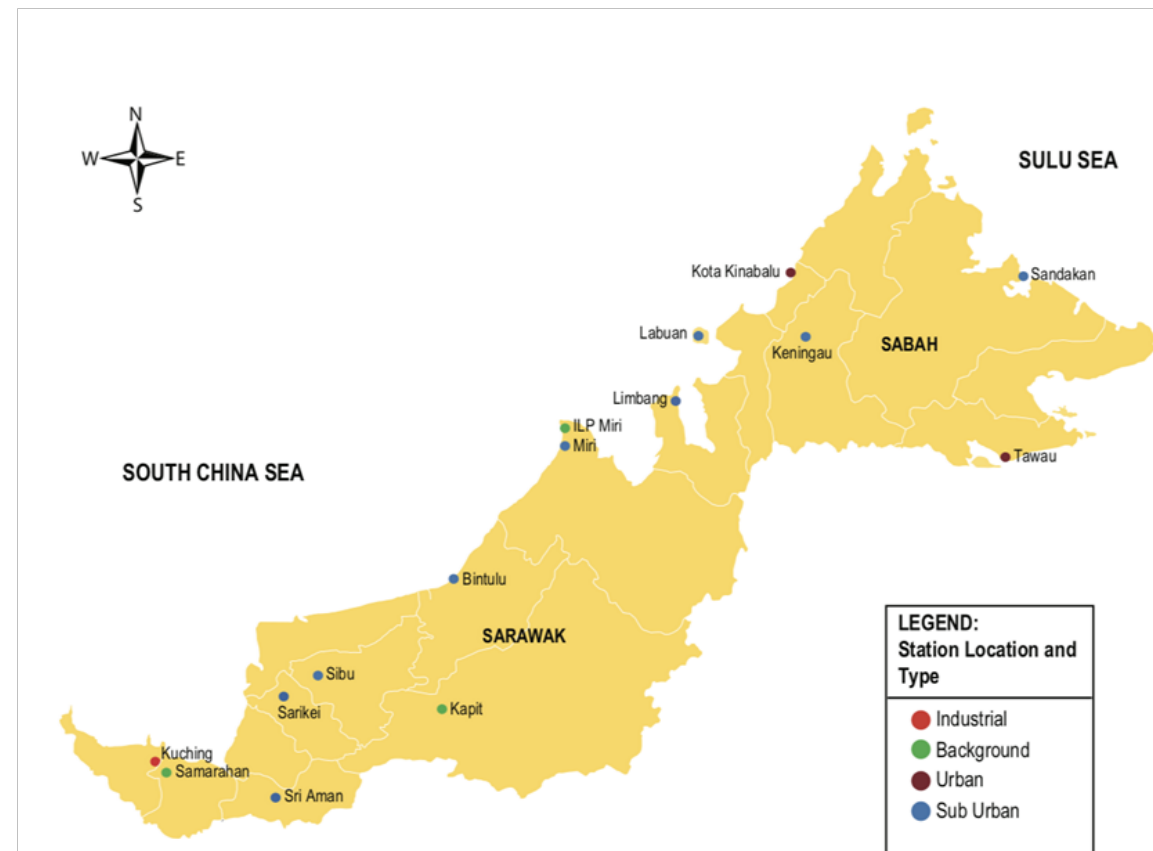
Air Monitoring Station

Continuous Air Quality Monitoring System (CAQM)



The Department of Environment (DOE) monitors ambient air quality through a network of 52 continuous monitoring stations. These monitoring stations are strategically located in urban, sub urban and industrial areas (to detect any significant change in the air quality which may be harmful to human health and the environment).

Distribution of station locations



ASMA Air Monitoring Station

Air Quality Monitoring Network



*ASMA = Alam Sekitar Malaysia

PM_{2.5} during Haze Episode

Physical & Chemical Properties during Haze

Aerosol Continuous Monitoring

- GRIMM EDM-SVC 365
- Flowrate of 1.2 L min^{-1}
- 1-min interval continuously
- 31 size channels : 265 – 34000 nm
- 2012 Jan – 2012 July
- Measuring principle: laser light scattering



PM_{2.5} Gravimetric Sampling

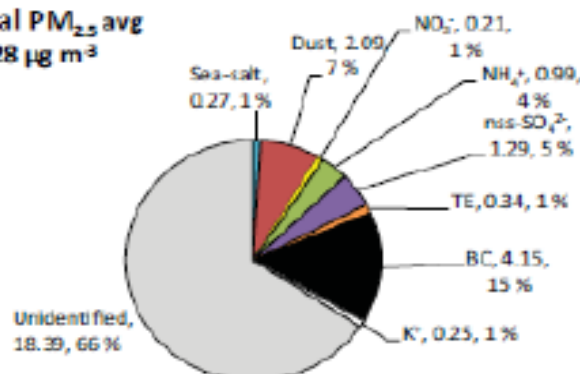
- Tisch HVS PM_{2.5}
- Flowrate of $1.13 \text{ m}^3 \text{ min}^{-1}$
- 24 h sampling/filter
- Quartz filter [Whatman QM-A; 8' X 10']
- 2011 August – 2012 July

Determination of PM_{2.5} sources – Haze and Non Haze

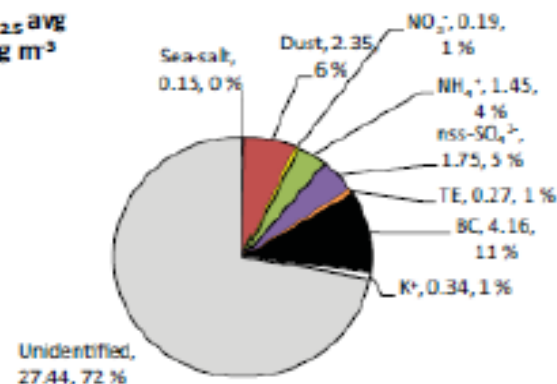
Physical & Chemical Properties during Haze Episode

(10)

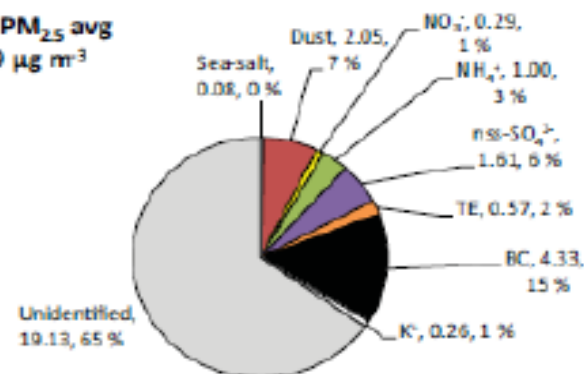
Annual PM_{2.5} avg
= 28 µg m⁻³



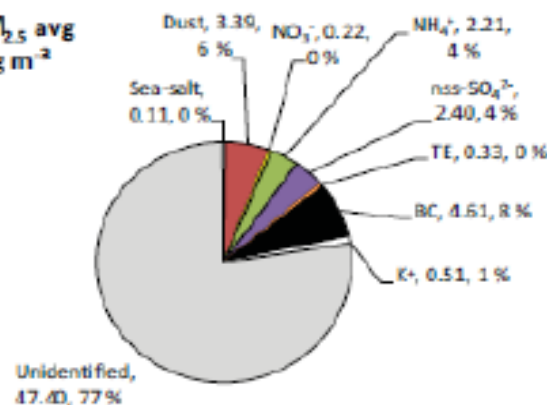
SW PM_{2.5} avg
= 38 µg m⁻³



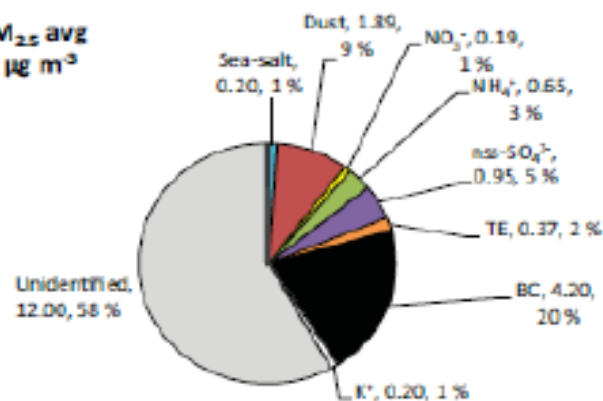
INT.2 PM_{2.5} avg
= 29 µg m⁻³



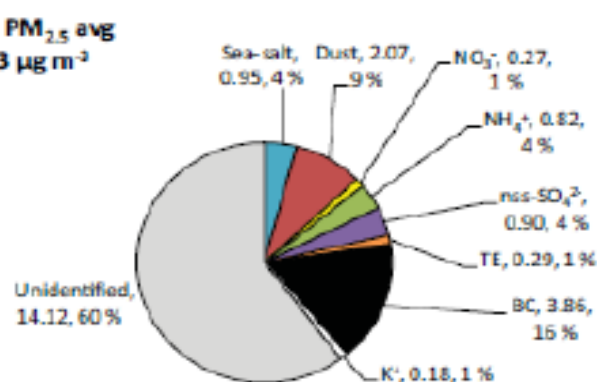
Haze PM_{2.5} avg
= 61 µg m⁻³



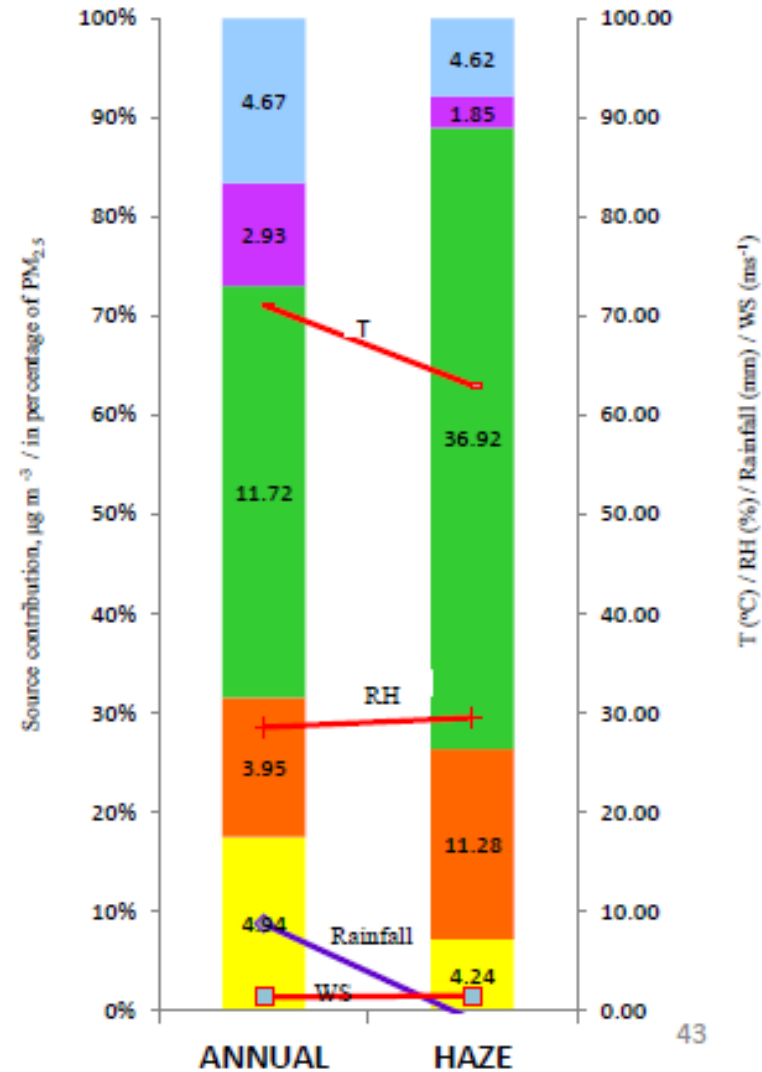
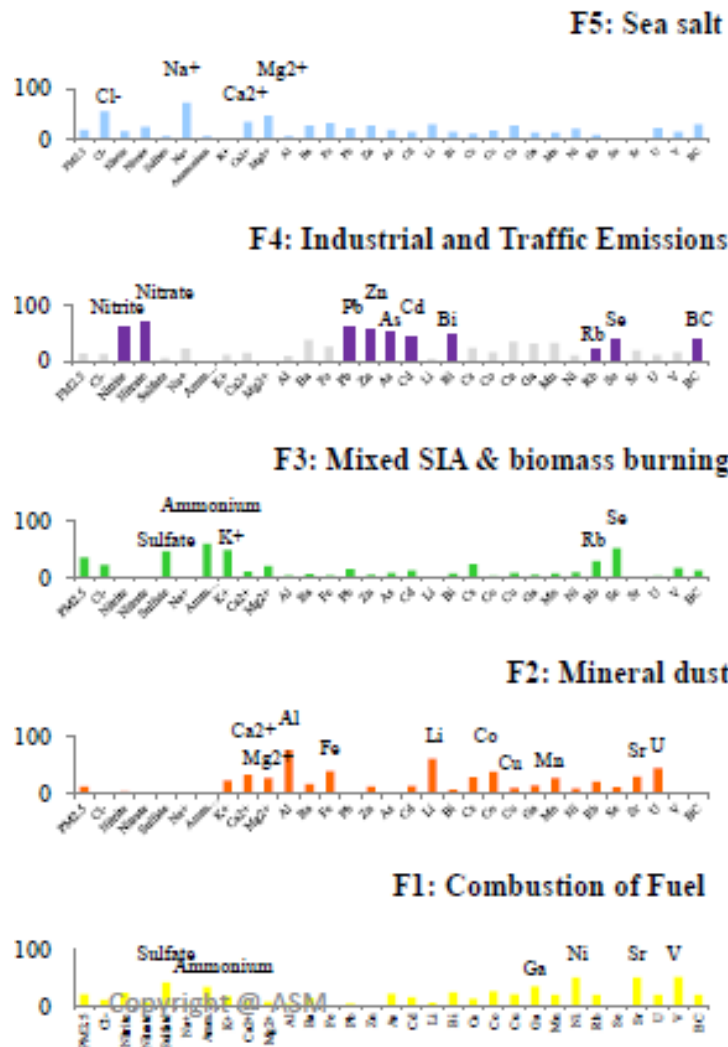
NE PM_{2.5} avg
= 21 µg m⁻³



INT.1 PM_{2.5} avg
= 23 µg m⁻³

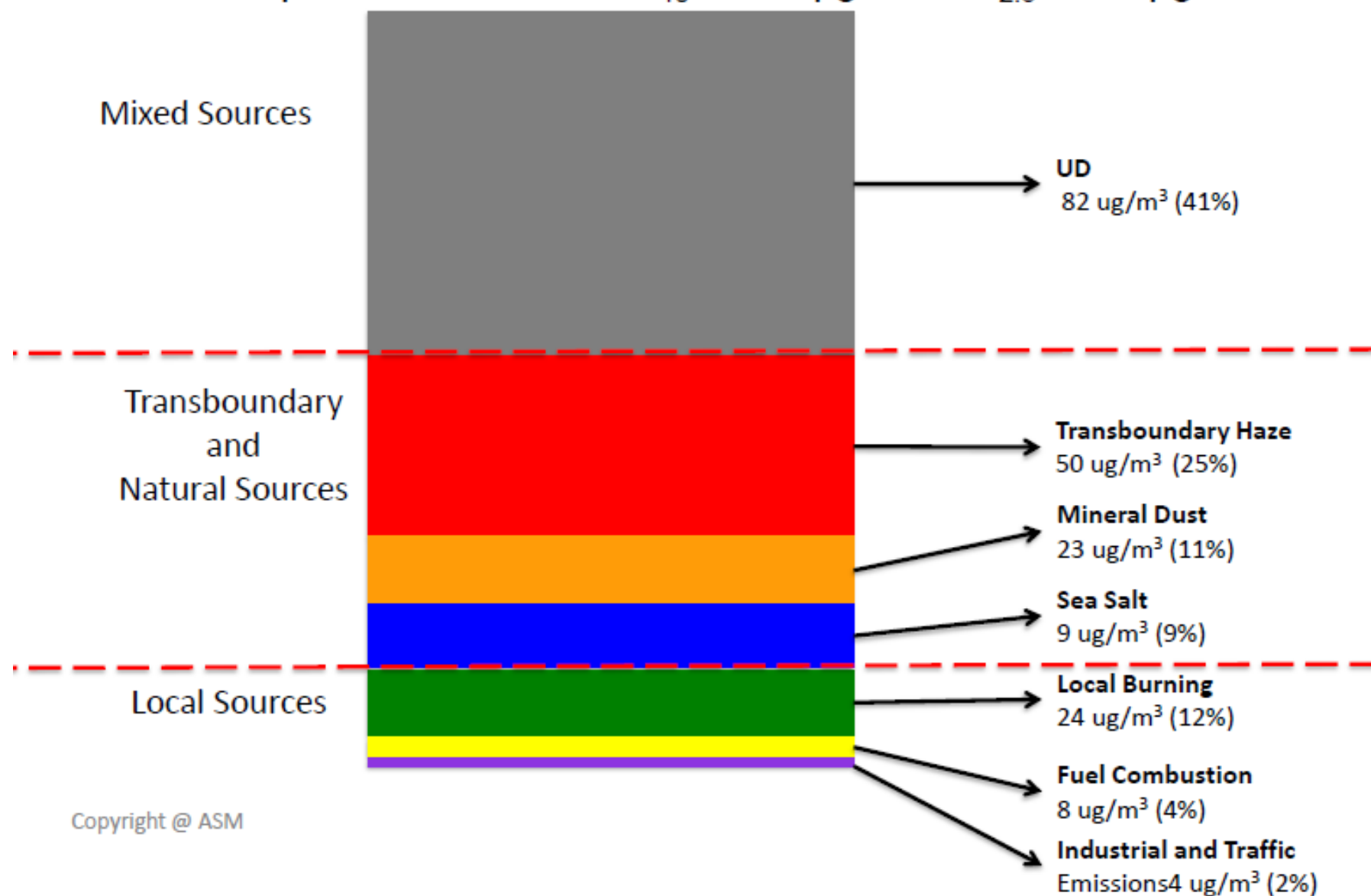


PMF-MLR Source apportionment: PM2.5 chemical composition (Inorganic & BC) Physical & Chemical Properties during Haze Episode



Determination of PM_{2.5} sources – Haze and Non Haze

Assumption if API is 300 $PM_{10} = 286 \mu\text{g}/\text{m}^3$, $PM_{2.5} = 201 \mu\text{g}/\text{m}^3$



Source of Air Pollution

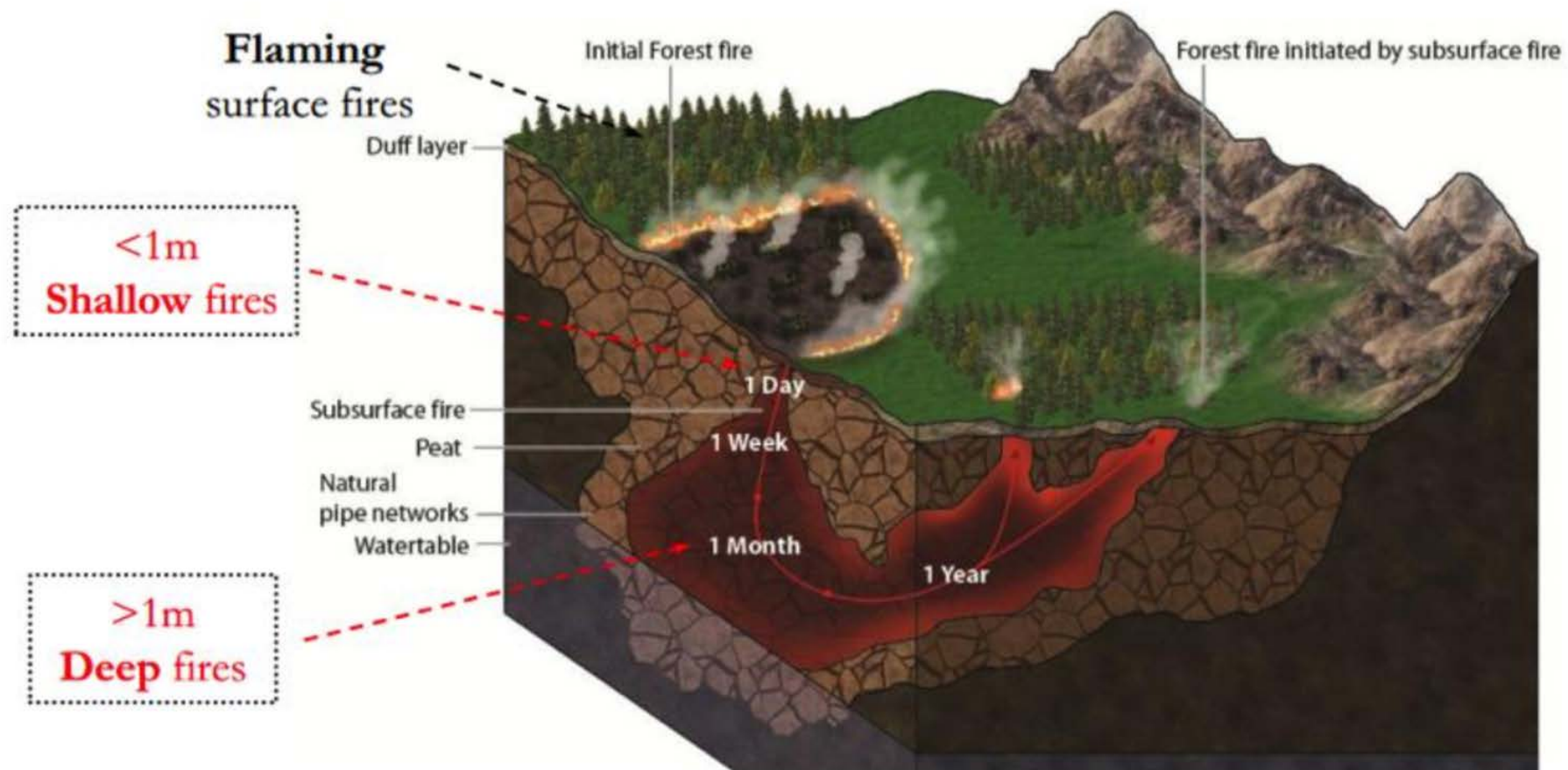
Land use
changes

Local
anthropogenic

Peat combustion

Slash and burn

Burning within
oil palm
plantation



Rein et al. (2008)

Haze: Bad new folks! Sumatra hotspots double to 118 on Saturday

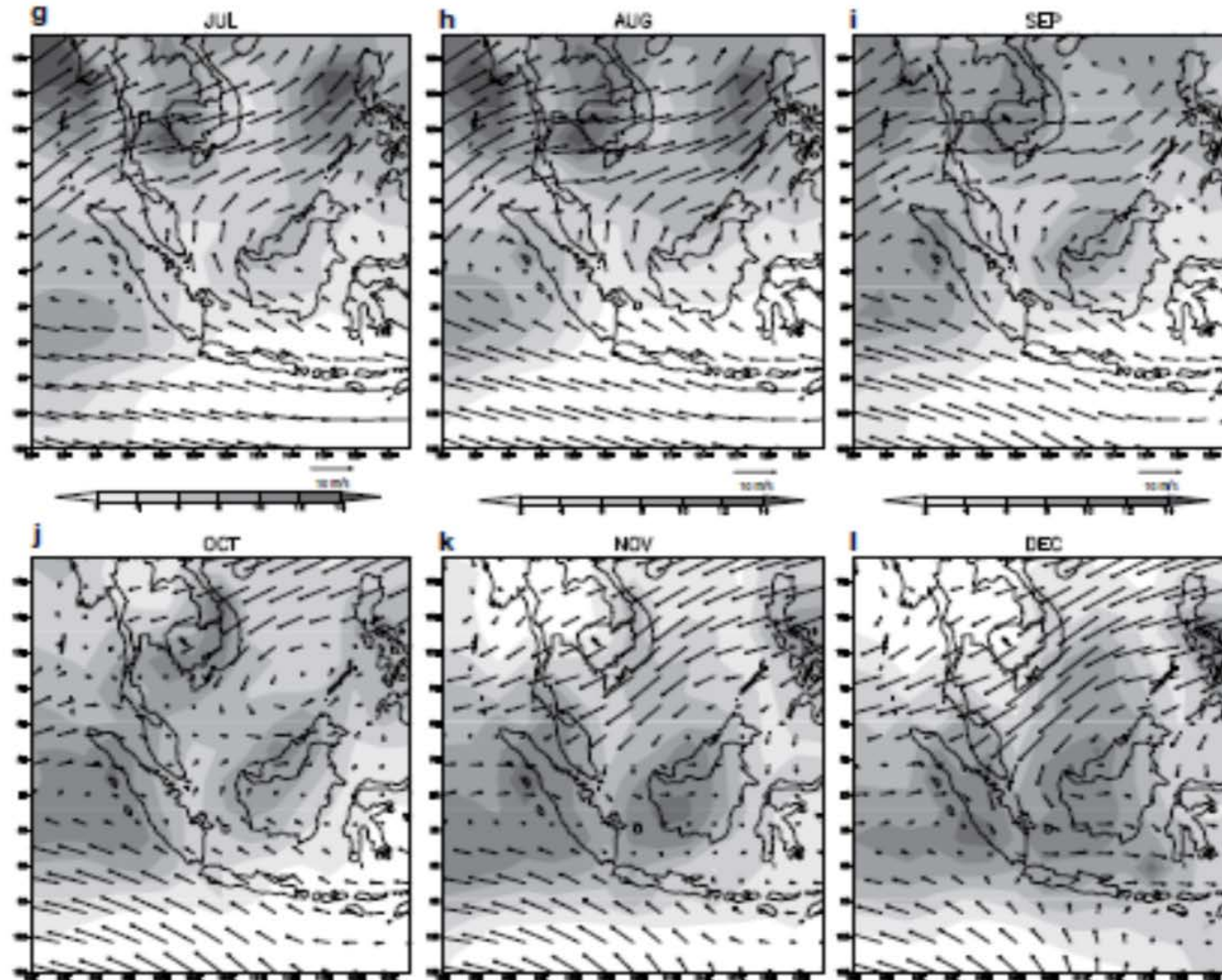
JUNE 23, 2013 BY ADMIN [LEAVE A COMMENT](#)



Flaming

Smouldering

WIND FIELDS

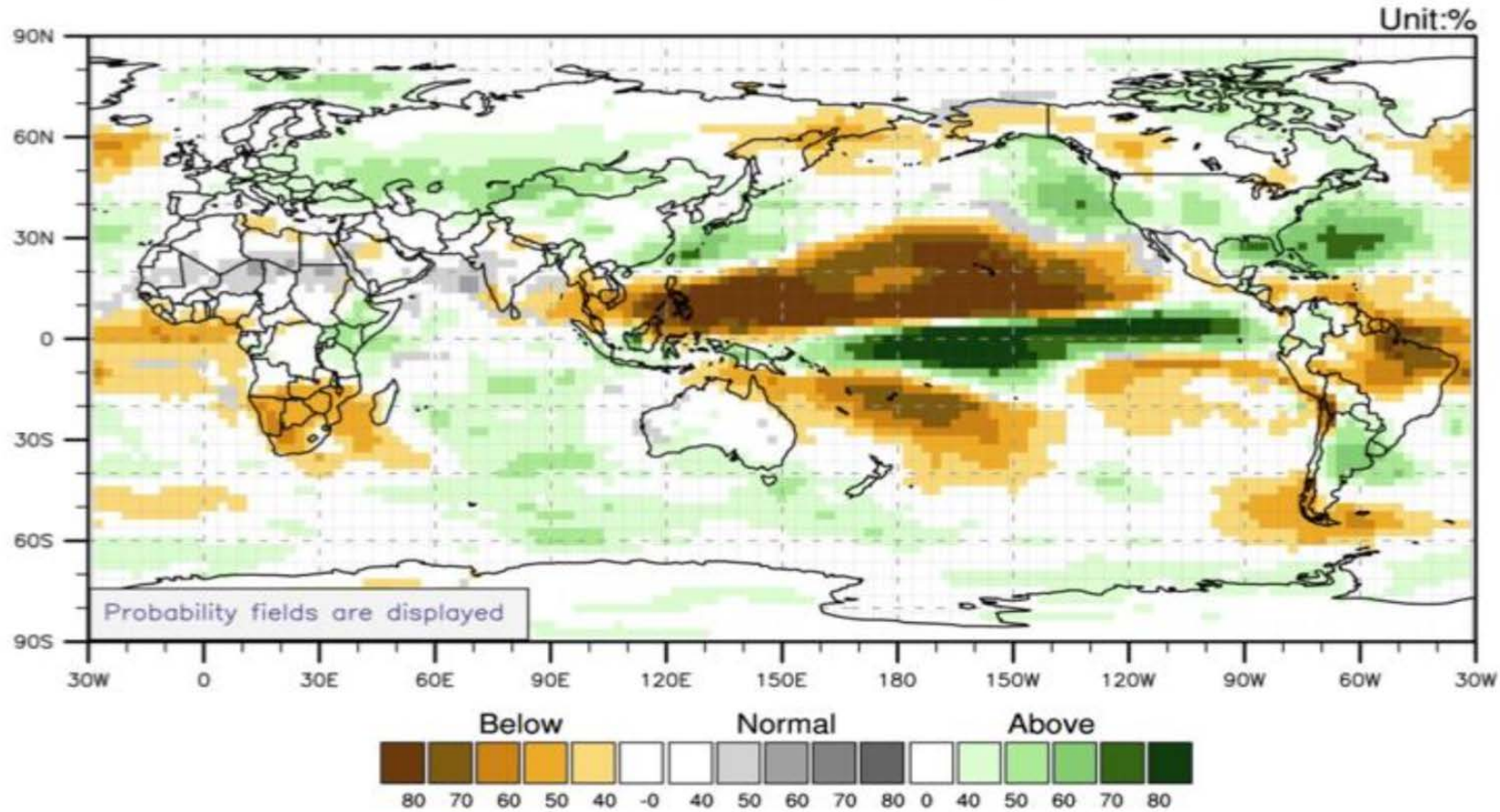


**Jun-to-Oct
Southwest
monsoon**

Correlation Maps

Forecastability

Precipitation for February-April 2016



Source of Aerosol Data

1

Ground based
monitoring

2

WMO Global
Atmospheric
Watch

3

Aeronet

4

Space borne
remote sensing

WMO Global Atmosphere Watch: Measurement Stations Worldwide

01



WMO Global Atmospheric Watch (GAW) Network of Stations)

01

Danum Valley, Sabah (1 station)

Tanah Rata in Cameron Highlands (2 regional station)

Petaling Jaya (1 station)

02

Regional stations:

- PJ stations measures TSP & PM10
- The samples are then sent for analysis to determine its chemical compositions
- To study urban air quality and meteorology and providing urban air pollution forecasts
- Tanah Rata stations includes Rainwater chemical composition, reactive gases, aerosol load and chemical composition, surface ozone and meteorology

03

Global station monitors background concentration of atmospheric parameters to study long-range transport of pollutions and ability of forecast to act as sinks for atmospheric pollutants

CHARACTERIZATION OF AEROSOL
OPTICAL PROPERTIES VARIABILITY
USING AERONET SUNPHOTOMETER
AND CLASSIFICATION OF AEROSOL
TYPES

4.1 Climatology Variations in Aerosol Optical Properties

- Four years observations of aerosol optical properties were carried out at the Kuching, Sarawak by using AERONET Sun-photometer data from August 2011 until December 2015.
- Long term measurements of aerosol optical depth (AOD), Angstrom exponent (α), single scattering albedo (SSA), asymmetry factor (ASY), refractive index and aerosol size distribution were analyzed and compiled to describe the climatology of the optical properties of aerosols in study area.
- The contribution of this climatology variations helps to gain knowledge on how aerosols might influence the regional radiation budget (Olcese et al. 2014). According to Garcia et al. (2008), the aerosols can influence the radiation budget by the interaction of aerosols with the solar radiation causes strong scattering and absorption mechanisms
- For that reason, different aerosol types will have different characteristics of scattering and absorption properties can leads to different effect on the estimation of aerosol radiative forcing (ARF) value.

STUDY SITE

The experimental site for this study is at Kuching, Sarawak. This region has high potential because of the high sources for pollution to occur and rapid urbanization and industrial expansion.

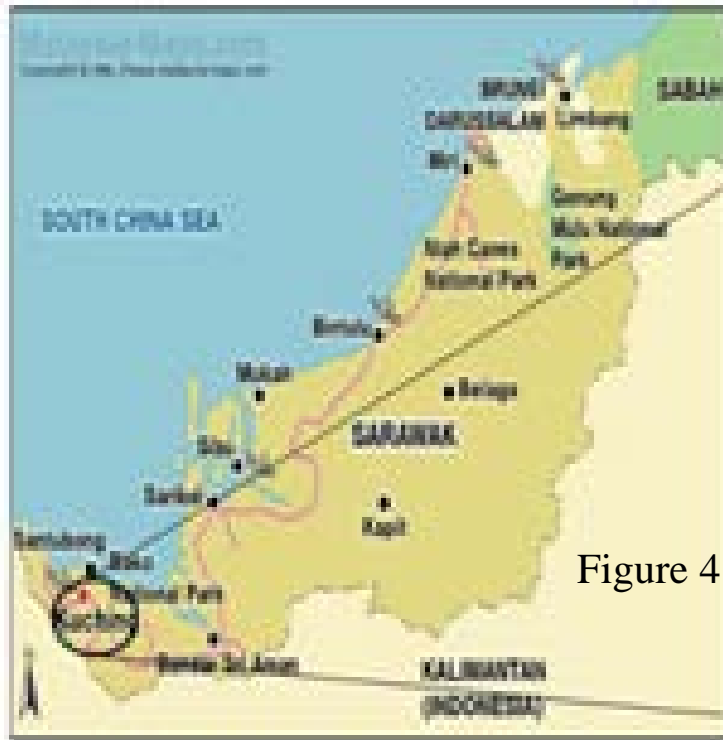


Figure 4.1: Study site of Kuching area

- As for the location of AERONET Sunphotometer at Kuching area, it is mounted at the Observation Tower of Kuching Meteorological Station located at the Kuching International Airport, Sarawak. The latitude for AERONET Sunphotometer is at 1.491°N and 110.349°E for the longitude with elevation at 28 meters



Figure 4.2: Location of AERONET Sunphotometer at Observation Tower of Kuching Meteorological Station

4.1.1 Aerosol Optical Depth (AOD)

- AOD indicates the concentrations of aerosol loading presence in the atmosphere either indicate lower or higher values.
- Ranjan et al. (2007) explained the characterization of AOD values at different wavelengths is very useful in gaining knowledge and understanding on the aerosol size distribution, seasonal variations of aerosols can be investigated and helps to identify the main sources of different types aerosol which presence in the atmosphere.

- The highest appearance of AOD was recorded during September 2015 at wavelength 440nm with 2.3354 ± 1.032 and December 2012 recorded the lowest AOD values with the range of 0.0321 ± 0.004 at 1020nm.
- The low concentration of AOD recorded at Kuching from November 2011 until April 2011 due to heavy rainfalls that probably washed away some of the aerosols and reduce the presence of aerosols in the atmosphere.
- High concentration of AOD observed from August 2012 to October 2012 maybe due to the presence of dry season, biomass burning activities from neighboring countries and urban activities.
- Low patterns of AOD distribution occurred during November to February for each year and high patterns of AOD distribution are observed from June to October yearly. Therefore, the trends for AOD variations are based on the seasonal monsoon weather.

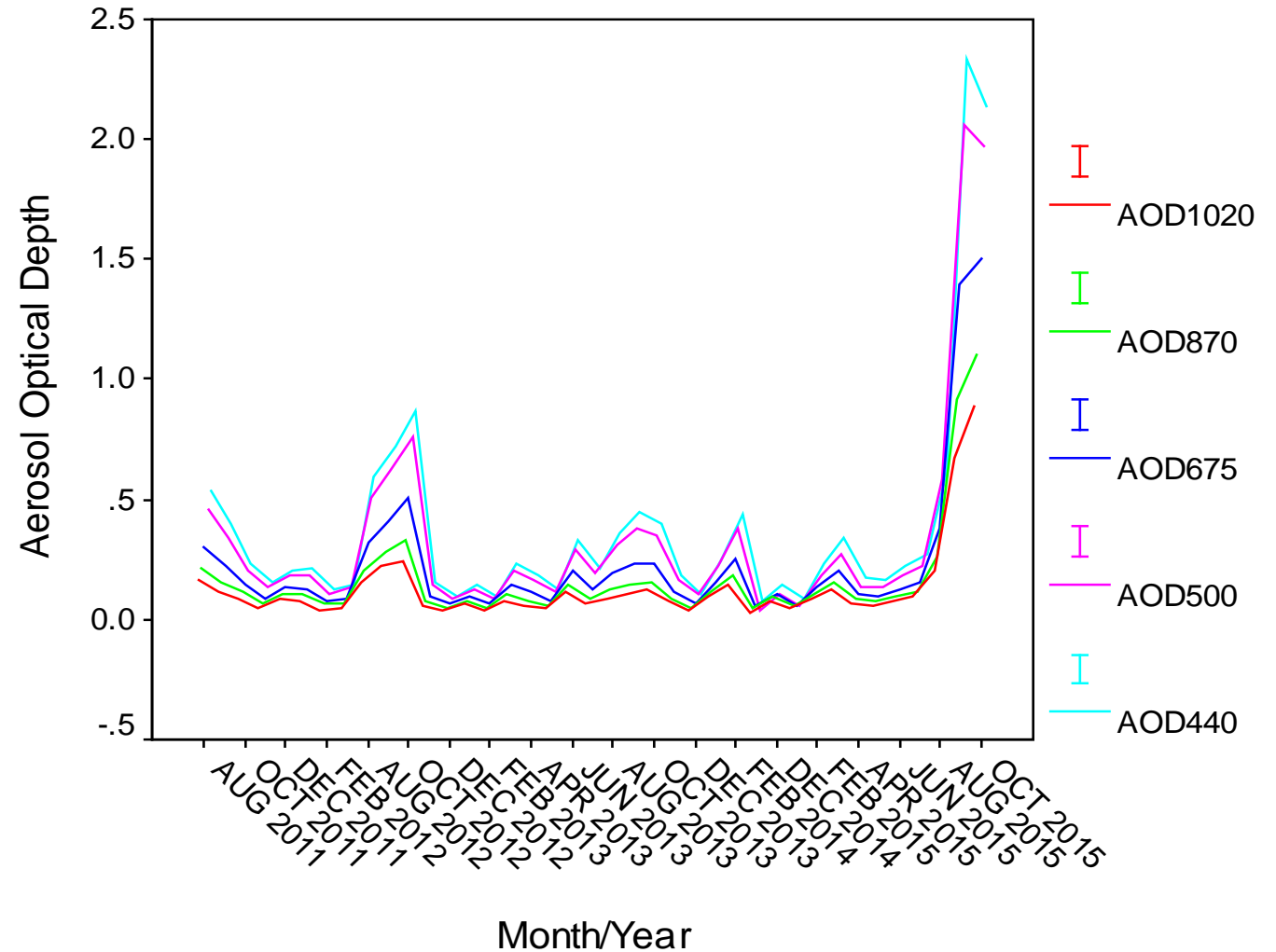


Figure 4.3: Monthly Variations of Aerosol Optical Depth at Five Different Wavelengths from August 2011 until December 2015

- For the investigation of the origins of the air masses arriving at Kuching area for the period of study due to long range transport, the back trajectory model was performed based on NOAA HYSPLIT model invented by Draxler and Rolph (2003).

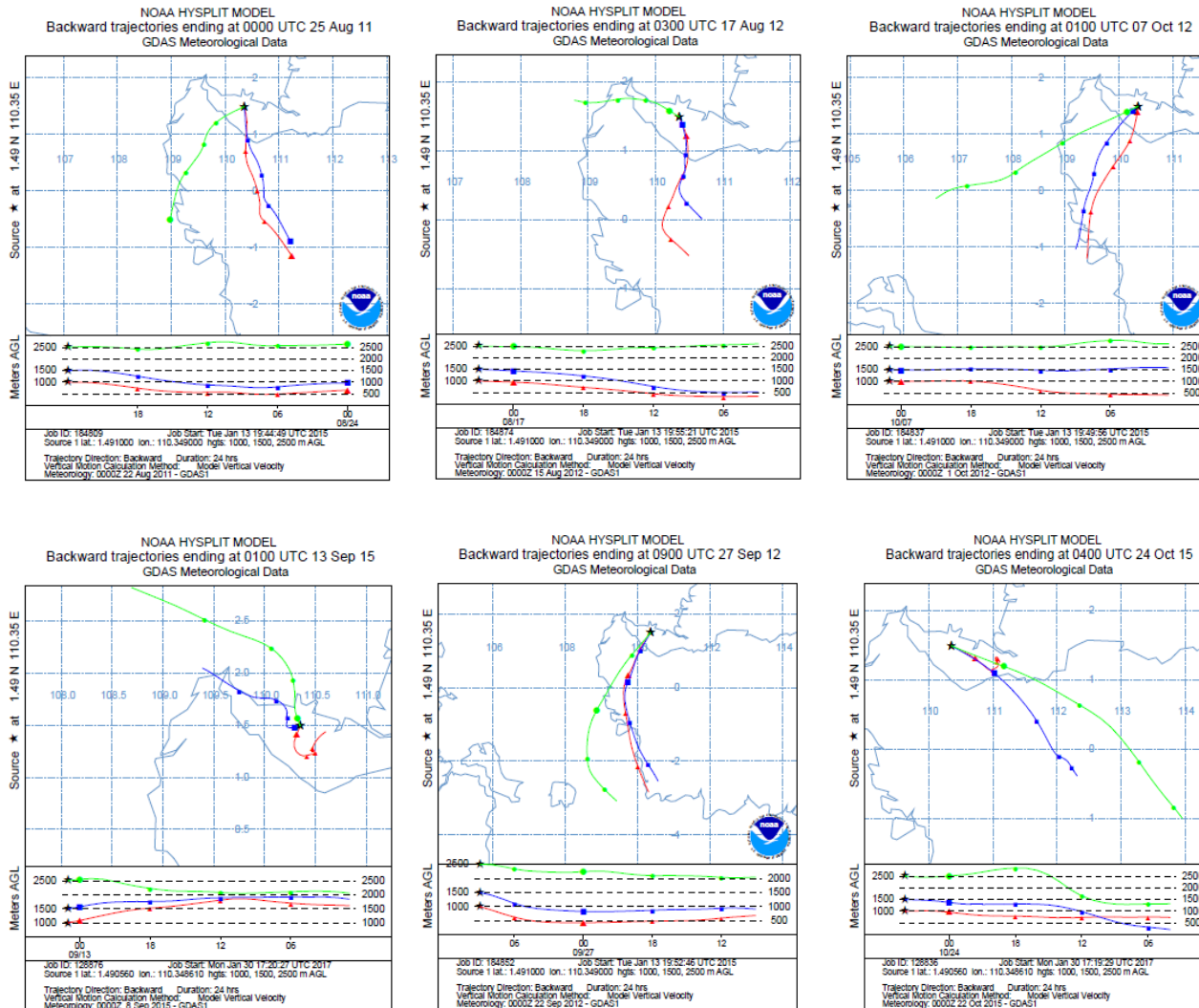


Figure 4.4: HYSPLIT Back Trajectory Model at 1000, 1500 and 2500m on Different Days from 2011 until 2015

The origin air masses reached Kuching comes from Sumatera (Indonesia), Central Kalimantan, Borneo (Indonesia), Java Sea and also from South China Sea.

The long range transport of aerosols is caused mainly from the forests fires and open burning continues to occur on the Indonesian islands in the dry season.

From Jun to September, Malaysia is affected by the southwest monsoon which causes the dry weather and the prevailing wind direction is generally blowing from Sumatra to Malaysia.

Same result was obtained from the study by Rahman et al. (2011) regarding the application of back trajectory model to predict long range transport of pollutant for Klang Valley. The observations clearly show that the forest fires in parts of Sumatra and Kalimantan which usually occurred from Jun to September is one of the probable key sources to the heavy haze phenomenon across Southeast Asia.

4.1.2 Angstrom Exponent (α)

- Angstrom exponent (α) is an informative parameter regarding aerosol size distribution either it shows the presence of fine mode aerosols or coarse mode aerosols.

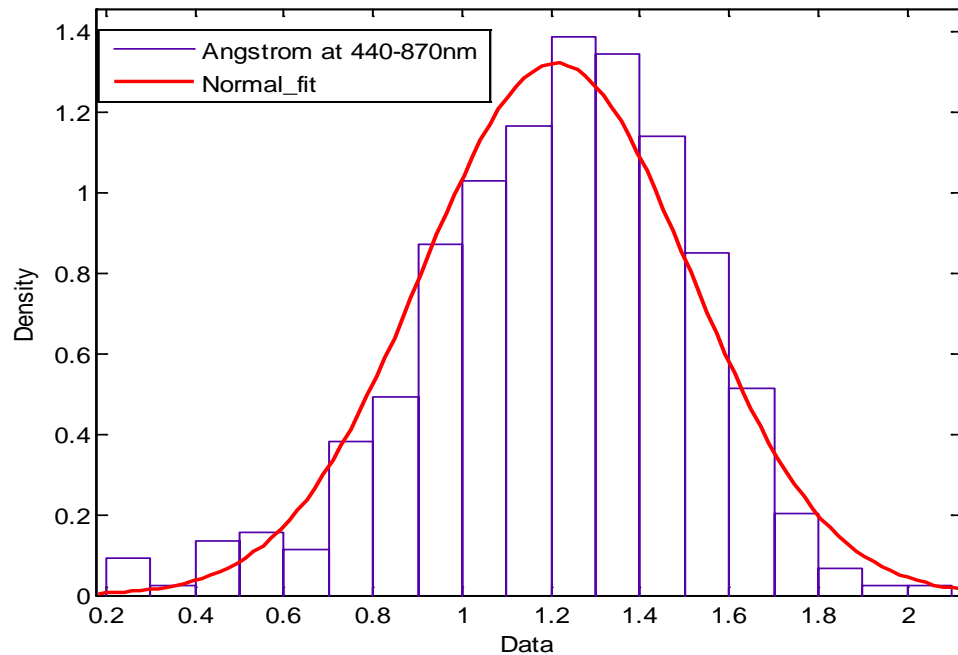


Figure 4.5: Normal Fitted Distribution for Angstrom Exponent at 440-870nm

It shows the normal fitted distribution for α value at 440-870nm where the mu value is 1.211 and the sigma is 0.302 with the equation presented in Equation 4.1.

$$f(x|\mu, \sigma) = \frac{1}{0.302\sqrt{2\pi}} e^{-\frac{(x-1.211)^2}{2(0.302)^2}}, -\infty < x < \infty \quad (4.1)$$

Balakrishnaiah et al. (2011) stated there are two modes of aerosols that usually occurred in study area dusty ($\alpha < 1$) and non-dusty ($\alpha > 1$) conditions.

It reveals a great dispersion of α values with obviously single peak distribution with the range varied from 0.2 to 2.2 and the peak is between 1.0 and 1.4.

High presence of fine mode aerosols ($\alpha > 1$) at Kuching area related to the mixture of urban or continental and biomass burning aerosols. As for the value of α lower than 1 represents the coarse mode particles consist of dust or maritime aerosols.

4.1.3 Single Scattering Albedo (SSA) and Asymmetry Factor (ASY)

- $\theta=180^\circ$ and the light is being scattered entirely in a forward direction ($\theta = 0^\circ$).
- SSA is the ratio of scattering to total extinction efficiency and both of the parameters provide information regarding scattering and absorption properties of different aerosol types (Alam et al. 2012).
- For SSA value is between 0 and 1 where value near to 0 indicates total absorption and SSA value near to 1 indicates total scattering.
- The range value for ASY is between -1 to 1 with ASY value near to -1 corresponds to back scattering direction with

- Most of the SSA value was higher than 0.8 and it shows that shorter wavelengths produced higher SSA value compared to longer wavelengths with the range value of SSA is between 0.8253 and 0.9837.
- SSA value was decreasing with increasing wavelength reflecting the dominance of urban or continental aerosols over Kuching with mostly the value for each month is higher than 0.9. As stated by Dubovik et al. (2002) when SSA value is between 0.9 to 0.8 it corresponds to the presence of urban and continental aerosols.
- October 2012 it is reported only slightly changes of SSA value when wavelength bands are increasing which concluded the presence of high sulfate or silicate particles (Verma et al. 2010).
- August 2011 there is drastically decreased of SSA value when wavelength band is increasing vary between 0.8253 at 1020nm and 0.9243 at 440nm which indicate highly absorbing aerosols which comes from local pollution such as urban aerosols or biomass burning aerosols (Bergstrom et al. 2007).

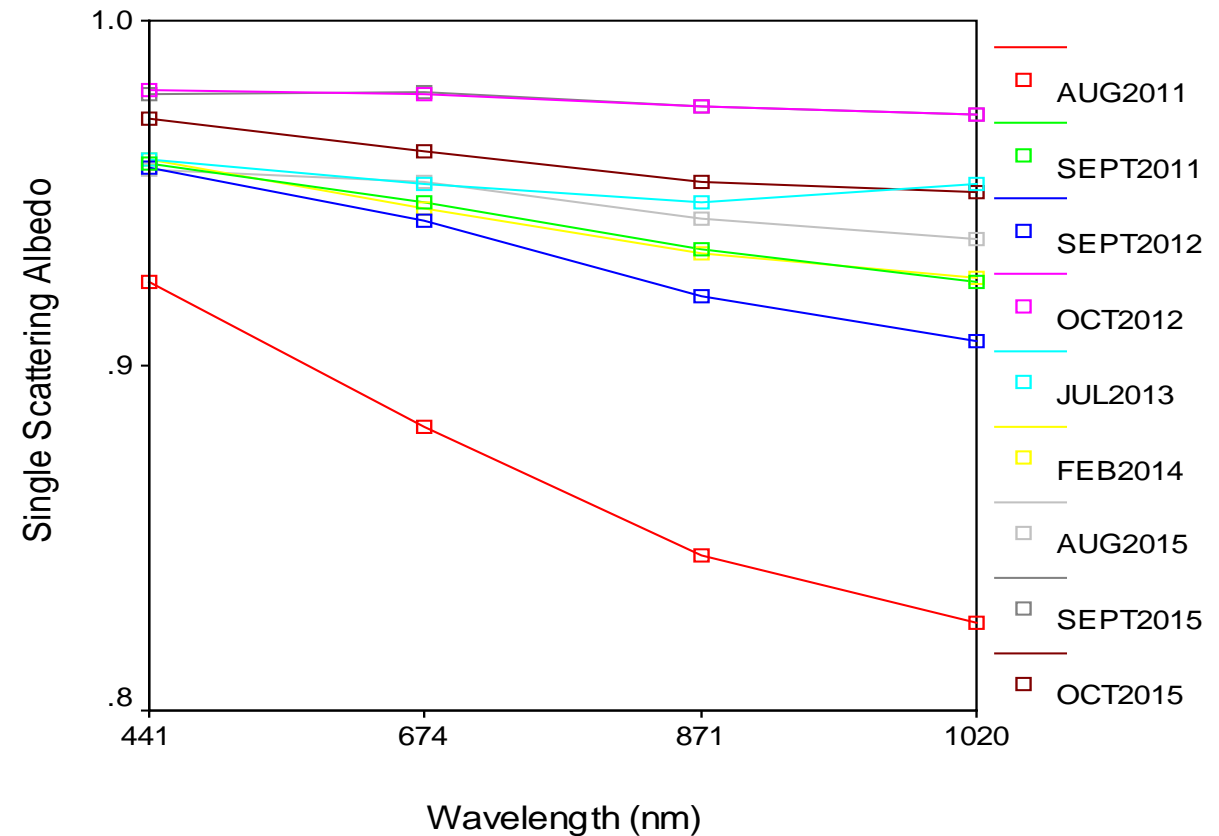


Figure 4.6: Monthly Variations for Single Scattering Albedo at Different Wavelengths from 2011 until 2015

- ASY value is decreasing with increasing wavelength bands which suggests dominance of fine mode aerosols and mostly the lights scattered in forward scattering aerosols
- Based on the graph presented in Figure 4.11, December 2014 shows the highest contribution of ASY value with 0.7652 at 441nm and the lowest value was obtained during July 2013 at 1020nm with 0.5087.
- Range of ASY between 0.64 and 0.83 with the averaged at 0.72 indicates for dry aerosol particles depending on the aerosol types and seasonal variability.
- Spectral variability of ASY recorded for September 2013, February and April 2015 shows a decrease in ASY in the visible region and then slightly increases in the near IR region. It is corresponding to the influence of coarse mode particles for those particular months

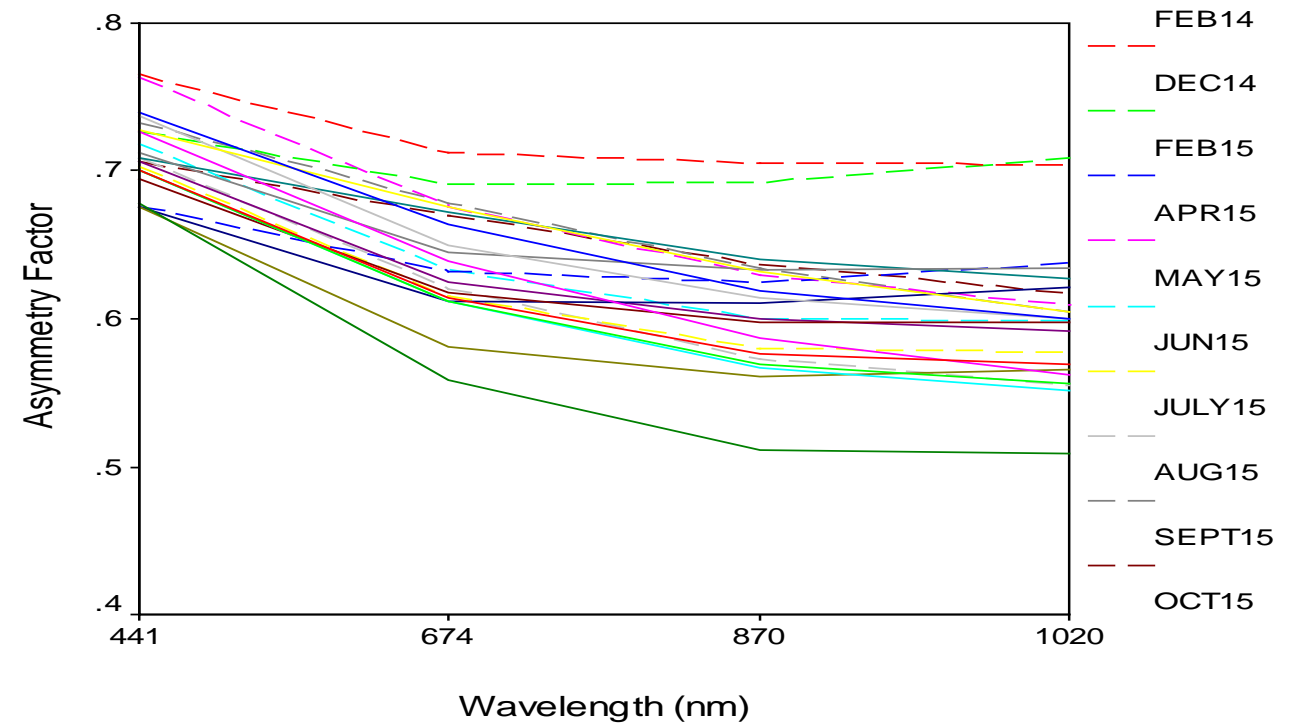


Figure 4.7: Monthly Variations for Asymmetry Factor at Different Wavelengths from 2011 until 2015

4.1.4 Refractive Index

- Refractive index provides information on physical and chemical composition of aerosols in the atmosphere.
- In refractive index, there are two parameters involves which are real part of refractive index ($n(\lambda)$) and imaginary part of refractive index ($k(\lambda)$).
- The real part refractive index corresponds to scattering properties of aerosols while imaginary part refractive index characterizes the degree of absorption for aerosol types (Bohren and Huffman, 1983; Alam et al. 2012).

- Range value for $n(\lambda)$ at available months is between 1.3556 and 1.5242 and mostly the $n(\lambda)$ is concentrated within 1.4 and 1.5. The lower value of $n(\lambda)$ consistent with the occurrence of anthropogenic aerosols such as urban and biomass burning aerosols (Yu et al. 2006).
- The occurrence for urban industrial aerosols at the study areas can be estimated with the $n(\lambda)$ value between 1.40 to 1.47. While for the biomass burning aerosols, the value of $n(\lambda)$ is the range from 1.47 and 1.51 and higher than 1.51 usually shows the presence for dust aerosols.
- Based on the result, it may not show a significant presence of dust aerosols because there are no drastically increase of $n(\lambda)$ was observed at near infrared wavelength band.

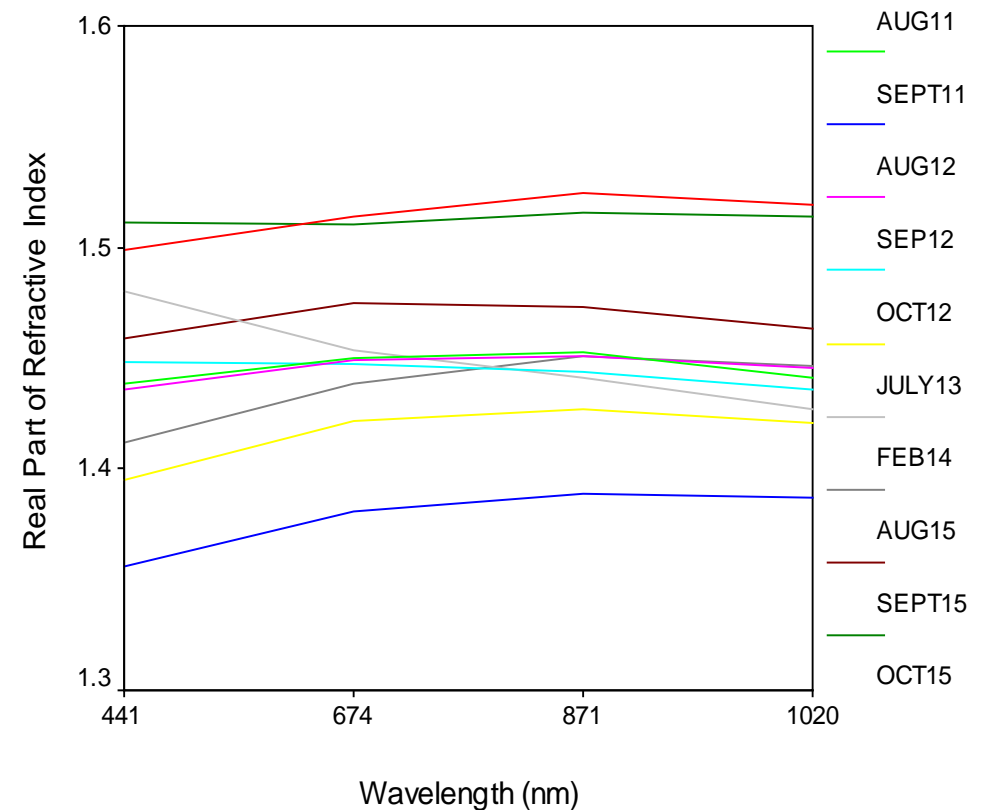


Figure 4.8: Monthly Variations for Refractive Index at Different Wavelengths from 2011 until 2015 for Real Part Refractive Index

- The range for $k(\lambda)$ value is between 0.001 to 0.01. The higher value for $k(\lambda)$ attributed to the influence of enhanced levels of anthropogenic absorbing particles released during the study period.
- Research study by Dubovik et al. (2002) where urban industrial aerosols had the range of $k(\lambda)$ value from 0.003 to 0.011 while for the presence of biomass burning 0.009 to 0.021.
- However, the estimation for the $k(\lambda)$ value for most of the monthly observations do not show any significant for spectral dependence and very low sensitivity to wavelengths with no clear pattern.

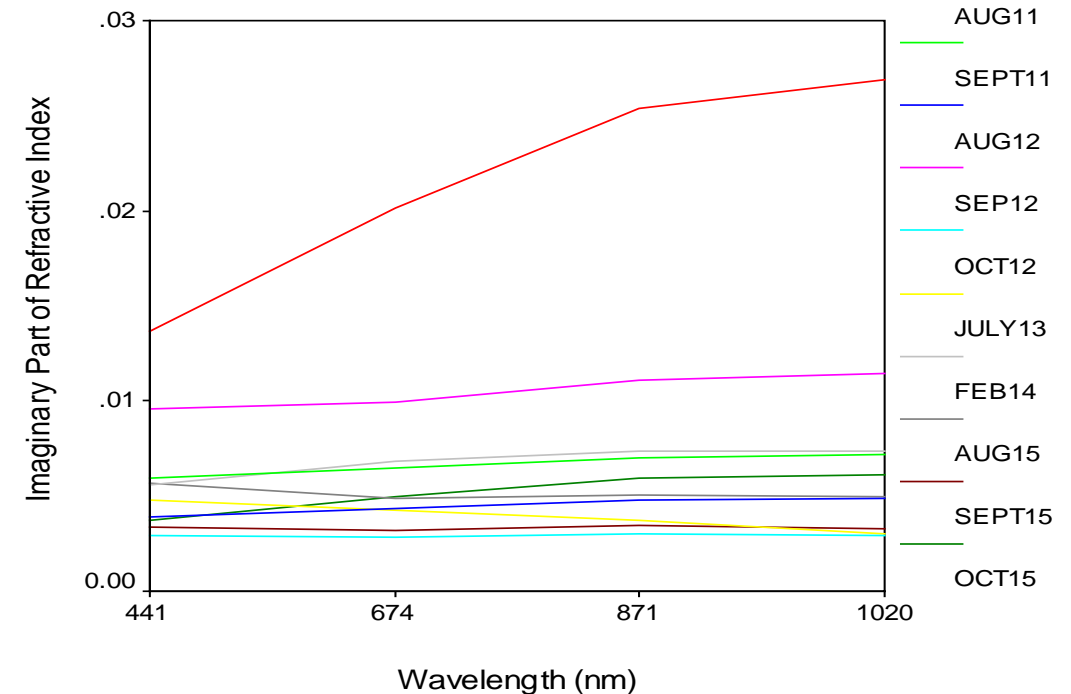


Figure 4.9: Monthly Variations for Refractive Index at Different Wavelengths from 2011 until 2015 for Imaginary Part Refractive Index

4.1.5 Aerosol Volume Size Distribution

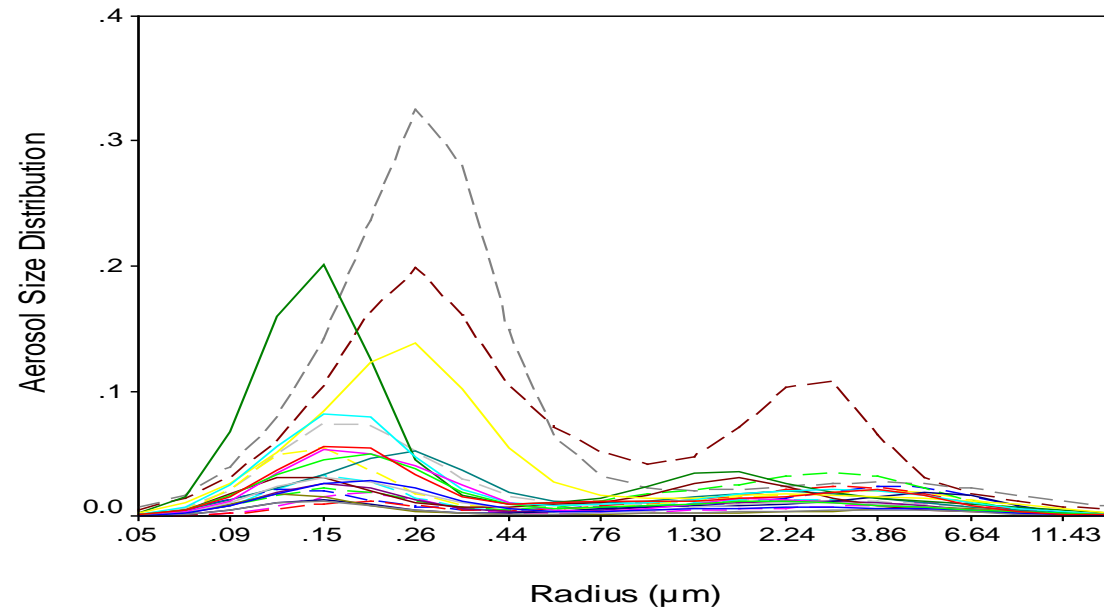


Figure 4.10: Monthly Variations for Aerosol Size Distribution Derived from Sky Radiance as a Function of Particle Radius

- It represents a bimodal lognormal distribution with fine mode dominating at a radius of about $0.15\mu\text{m}$, whereas the coarse mode is dominant with a radius at $3.86\mu\text{m}$.
- There are two distinct mode of aerosols occurred which are fine mode at $<0.6\mu\text{m}$ and $>0.6\mu\text{m}$ is for coarse mode aerosols.
- The fine mode size distribution indicated that during July 2013 the fine peak radius higher at $0.14\mu\text{m}$ while for September 2015, October 2012 and 2015 indicated at $0.25\mu\text{m}$. The higher values shows the frequent biomass burning activities, forest fire events and also related to human activities.

4.2 Classification of Aerosol Types

- categorized the aerosols in the atmosphere into four major types according to their radiation absorptivity and size. It can be divided into carbonaceous (absorbing fine mode), soil dust (absorbing coarse mode), sulfate (non-absorbing fine mode), and sea salt (non-absorbing coarse mode) (Higurashi and Nakajima (2002) .
- Different types of aerosol can be classified by using various measurements by such as analyzing the chemical composition of the aerosols or form a relationship between optical properties parameters such as AOD, α and SSA.
- Particularly, in this study the technique used to classify aerosol types over Kuching area is by using threshold criteria analysis.

4.2.1 Aerosol Optical Depth and Angstrom Exponent

- The purpose of using AOD and α parameter it will help to identify aerosol types based on frequency distributions of AOD and aerosol size distribution. This is because AOD value gives the information regarding aerosol loading while α is related to the aerosol size therefore the joint analysis for both parameters can have a better interpretation and understanding of data.
- In this analysis, AOD at two different wavelength bands are used firstly is at 500nm because optically 500nm is an effective visible wavelength that is very suitable for aerosol characteristics study (Stone et al. 2002; Tan et al. 2015) and give more clarification on fine mode aerosols (Ranjan et al. 2007).
- The other one is AOD at 870nm because as explained earlier in AOD variations at different wavelengths 870nm is very usefull to classify coarse mode aerosols (Toledano et al. 2007).

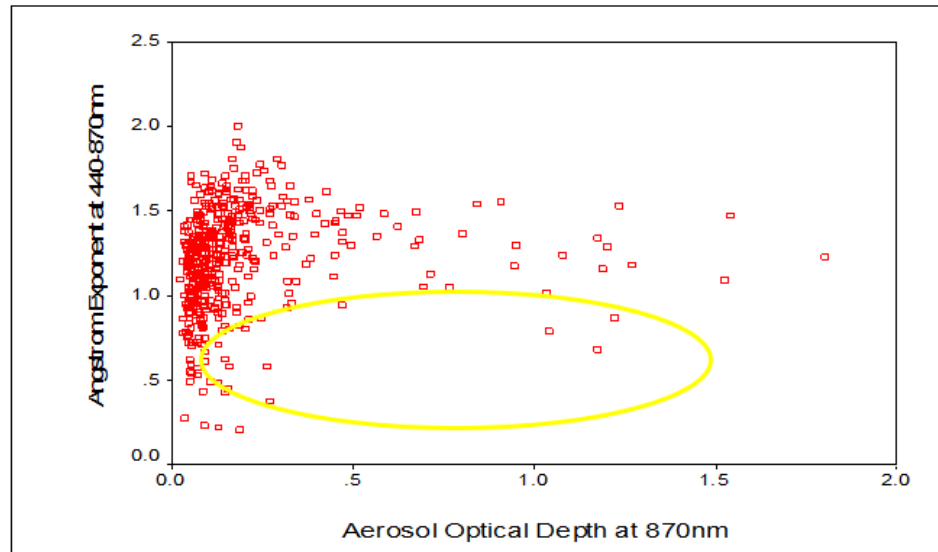
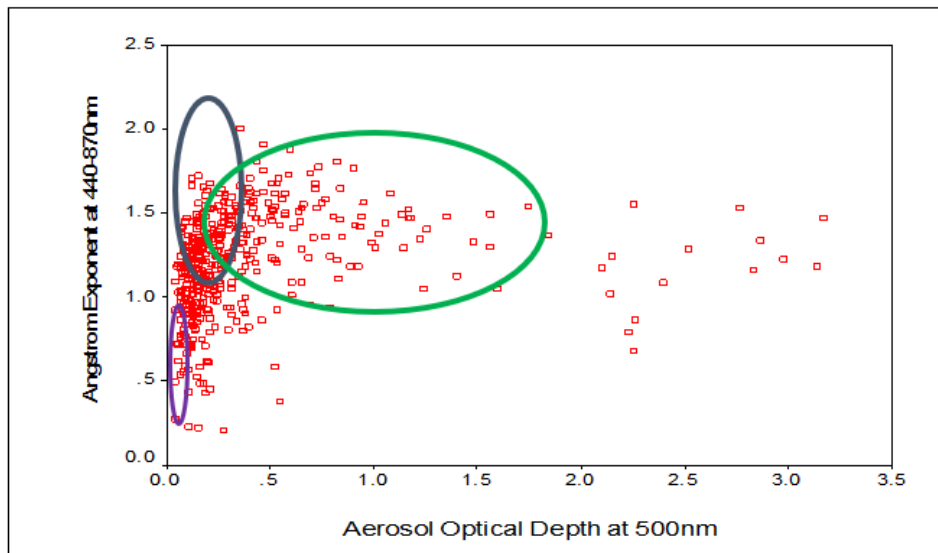
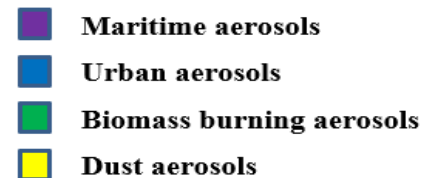


Figure 4.11: Scatter Plot of Aerosol Optical Depth and Angstrom Exponent for Aerosol Classification Types

- It shows that mostly the value is concentrated below 0.5 for AOD and below 1.5 for α .
- According to Toledano et al. (2007), the presence of pure maritime aerosols should be analyzed at the region with AOD at 440nm below than 0.2 and α is between 0 and 2 in the scatter plot while for Salinas et al. (2009) AOD at 440nm observed below than 0.15 and value for α at the range of 0.5 to 1.7.
- While the proposed threshold value for maritime aerosols in this study is $AOD \leq 0.1$ and $\alpha \leq 0.9$. The allocation for maritime aerosols can be seen in purple color.
- Based on the proposed threshold values, most of the value was highly concentrated at $AOD \leq 0.4$ and at α value ≥ 1.2 and with this result it indicates the presence of urban aerosol (blue color).
- Another circle is in green color which contributes to the presence of biomass burning aerosol with $AOD \geq 0.4$ and $\alpha \geq 1$.
- At AOD more than 0.2 and α less than 0.8 show the identification of dust aerosols with yellow circle in color.



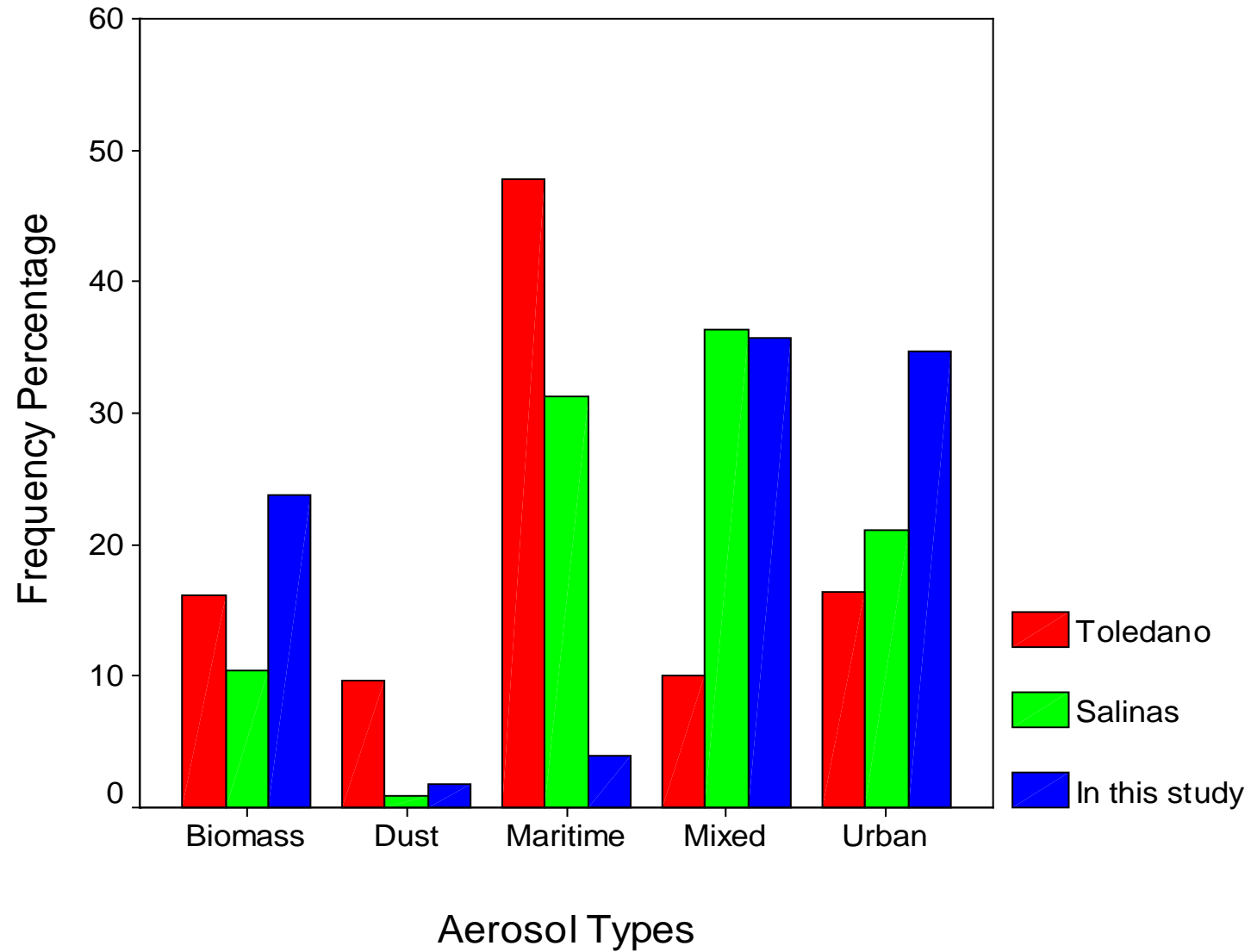


Figure 4.12: Frequency Percentage Distributions for Different Aerosol Types Based on Proposed Threshold Criteria

- The threshold value proposed by Salinas et al. (2009) does not correspond entirely to the range of threshold used in our study which shows less occurrence for urban and biomass burning aerosols with only 21.1% and 10.4%, respectively at AOD 500nm.
- As compared with the study by Toledano et al. (2007) where by using their threshold, it can be found that the amount of biomass burning aerosols recorded was 16.2% while for urban aerosols it was reported as 16.4% only.
- However, by using the threshold criteria value proposed from this study high frequency percentage for biomass burning aerosols was observed with 23.8% and quite high percentage at 34.7% for urban aerosols. There is consistency with the occurrence of haze that usually happens to Kuching area yearly produced by active burning in local and neighboring countries. These results are consistent with the records obtained from the Malaysian Meteorological Department, MET (2016). The high presence of urban and continental aerosols is due to the location of Kuching area as where rapid urbanization is developing.
- The appearance of dust aerosols shows for Toledano et al. (2007) only 9.6% and when using the threshold value from Salinas et al. (2009) the frequency percentage is 0.9%. By using the value obtained from this analysis, the dust aerosols recorded at 1.8%. High percentage of maritime aerosols was reported with 47.8% for Toledano et al. (2007) and 31.3% for Salinas et al. (2009). Fortunately, the lowest frequency percentage was obtained when using the proposed threshold values with only 4%.
- Based on the testing results indicate that the threshold criteria by Toledano et al. (2007) were quite reliable to use for the classification of aerosols types due to the minimal occurrence value of the indistinguishable aerosols which referred as mixed aerosol types. However, the threshold value do not show strong classification for urban and biomass burning aerosols. Therefore, the proposed threshold value retrieved from this study can be used to detect high presence of urban with $AOD \leq 0.4$ and $\alpha \geq 1.2$ and for biomass burning aerosols the AOD value ≥ 0.4 with high value of α ($\alpha \geq 1.0$) even though there are some presence of mixed aerosols. It can be concluded that urban and biomass burning aerosols are dominating at Kuching area.

4.2.2 Aerosol Optical Depth, Angstrom Exponent and Asymmetry Factor

- In this study, proposed of aerosol classification of aerosol types based on AERONET Sun photometer data by including the combination of AOD, α and ASY value.
- The combination of these three parameters help to classify different types of aerosols based on aerosol loading, size of aerosol particles and the scattering direction of aerosols.
- As stated by Srivastava et al. (2011), the ASY parameter is a very important parameter because it regulates the aerosol radiative forcing and as similar with SSA, ASY value is also dependent on the size and composition of aerosol particles (Ramachandran and Rajesh (2008); Srivastava et al. 2011).

- The highest percentage observed was for urban aerosols with 39% followed by mixed aerosols at 27%, 20% for biomass burning aerosols, 11% for maritime aerosols and lastly dust aerosols was observed at 3%.
- When using the relationship between three parameters it will help to reduce the observations for mixed aerosols types from 35.7% to 27%.

Figure 4.13: Different Types of Aerosol Classification Based on Relationship between Aerosol Optical Depth, Angstrom Exponent and Asymmetry Factor

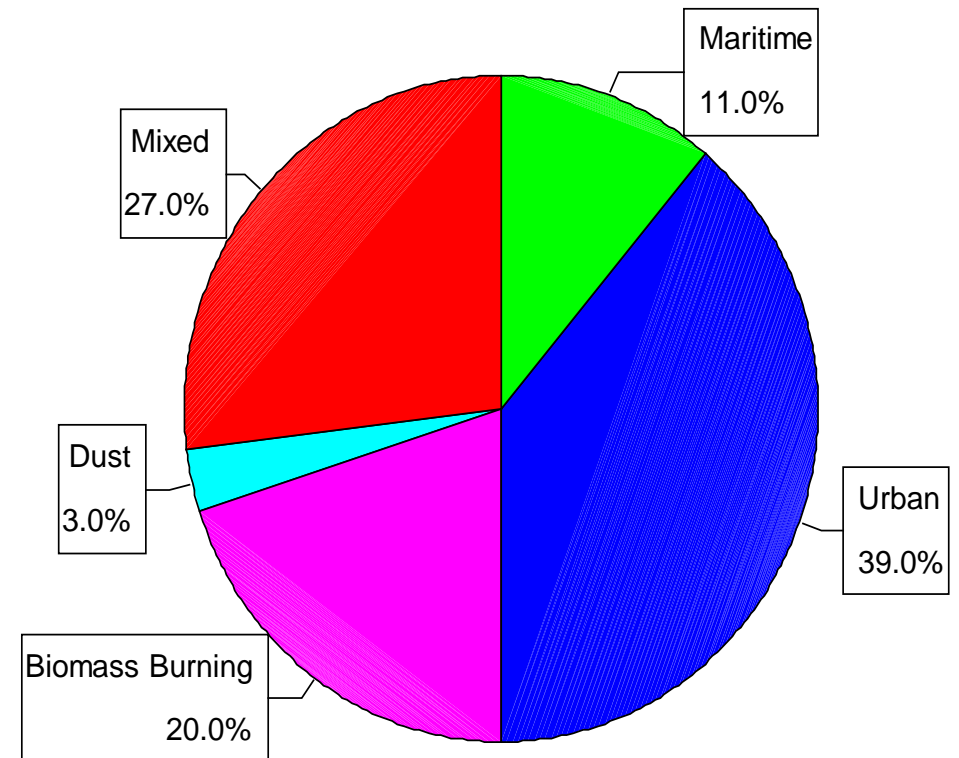


Table 4.1

Percentage Comparison for Different Types of Aerosols by Using Different Optical Properties

Aerosol Types/Parameters (%)	AOD and α	AOD, α , and ASY
Urban Aerosols	34.7	39
Biomass Burning Aerosols	23.8	20
Maritime Aerosols	4.0	11
Dust Aerosols	35.7	27
Mixed Aerosols	1.8	3

It can be concluded that the proposed aerosol classification algorithm by using three parameters which are AOD, α , and ASY also can be used to classify different types of aerosols. From the information obtained from ASY value, it will support the presence of different types of aerosols at that particular area.

**SPATIAL DISTRIBUTIONS AND
TEMPORAL VARIATIONS OF AEROSOL
OPTICAL DEPTH USING MODIS DATA**

DATA ACQUISITION

```
graph TD; A[DATA ACQUISITION] --> B[Moderate Imaging Resolution Spectroradiometer (MODIS)]; A --> C[Aerosol Robotic Network (AERONET) Sunphotometer];
```

Moderate Imaging Resolution Spectroradiometer (MODIS)

- Terra MODIS data Level 2 (Collection 5) and the code is MOD04.
- The MOD04 product provides global AOD over land and ocean with spatial resolution of 10km x 10km

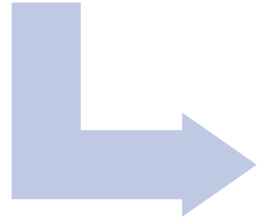
Aerosol Robotic Network (AERONET) Sunphotometer

- Ground based monitoring aerosol that can assess aerosol optical properties and to validate satellite retrievals of aerosol optical properties.
- Level 2 AOD retrieval from 500nm only was used for the analysis

METHODOLOGY

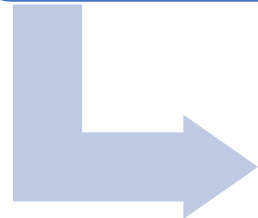
Spatial and temporal averaging

- Time window of ± 20 min
- Spatial average from pixels lying in $\pm(1/4^\circ)$

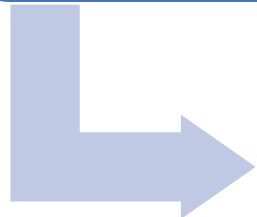


Retrieval of AOD

- Minimum Distance Technique
- Multiple Plane Regression Technique
- Artificial Neural Network



Interpolation Technique



Least Square Regression Technique

Interpolation Technique

- The AOD_{MODIS} data was at the wavelength range 550nm while $AOD_{AERONET}$ was at 500nm. For easy comparison with AOD_{MODIS} , $AOD_{AERONET}$ were interpolated by using Equation 3.

$$AOD_{550nm} = AOD_{500nm} \left(\frac{550}{500} \right)^{-\alpha} \quad (3)$$

- Where α is the angstrom exponent at wavelength 440/870nm obtained from AERONET data. After that, the relationship between AOD_{MODIS} is established with $AOD_{AERONET}$ based on least square regression and its output presented in correlation coefficient (R^2).

5.1 Minimum Distance Technique

- Minimum distance technique was performed for MODIS data to calculate the closest pixel of latitude and longitude to the AERONET site and the output were given in column and row pixel. The equation for minimum distance technique in the following way:

$$[R, C] = \left(\min \left[((x - x_1)^2 + (y - y_1)^2)^{\frac{1}{2}} \right] \right) \quad (1)$$

- Based on Equation 1, x is a longitude for MODIS and AERONET and y is the latitude for MODIS and AERONET. Smaller window sizes (11 x 11 pixels) are used to reduce undesirable errors due to topographic or aerosol types heterogeneity.

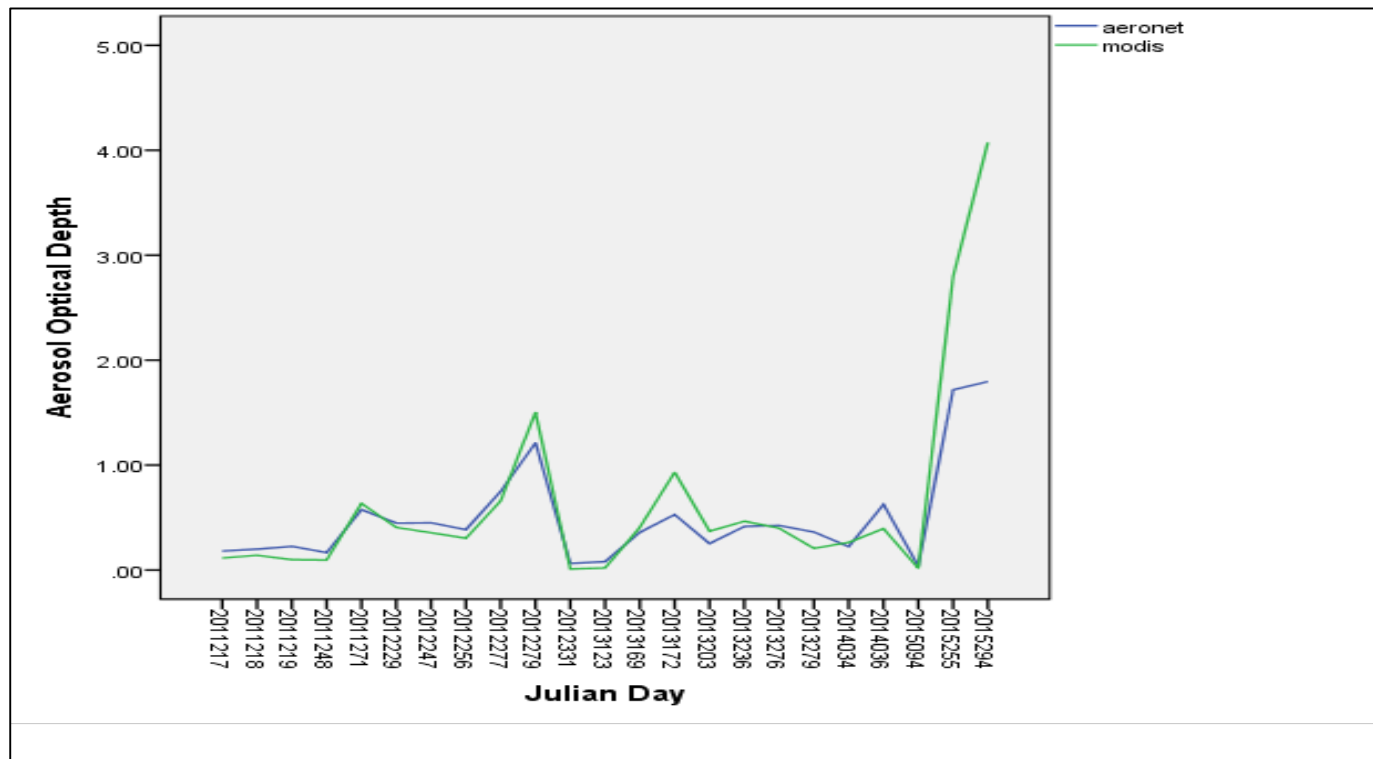


Figure 5.1: Variations for Aerosol Optical Depth for MODIS and AERONET using Minimum Distance Technique

- The minimum and maximum $AOD_{AERONET}$ value is 0.038 and 1.795, respectively.
- For the AOD_{MODIS} the value range between 0.01 and 4.075. Basically, the AOD value obtained is below than 2 however there are extremely high value of AOD_{MODIS} was retrieved at Julian Day 294 in 2015 with 4.075 while for $AOD_{AERONET}$ the value obtained was only 1.795.
- The reason for the overestimation of AOD_{MODIS} may come from dry season in Kuching area causes surface to become dry thus leads to higher value for surface reflectance (Tripathi et al., 2005).

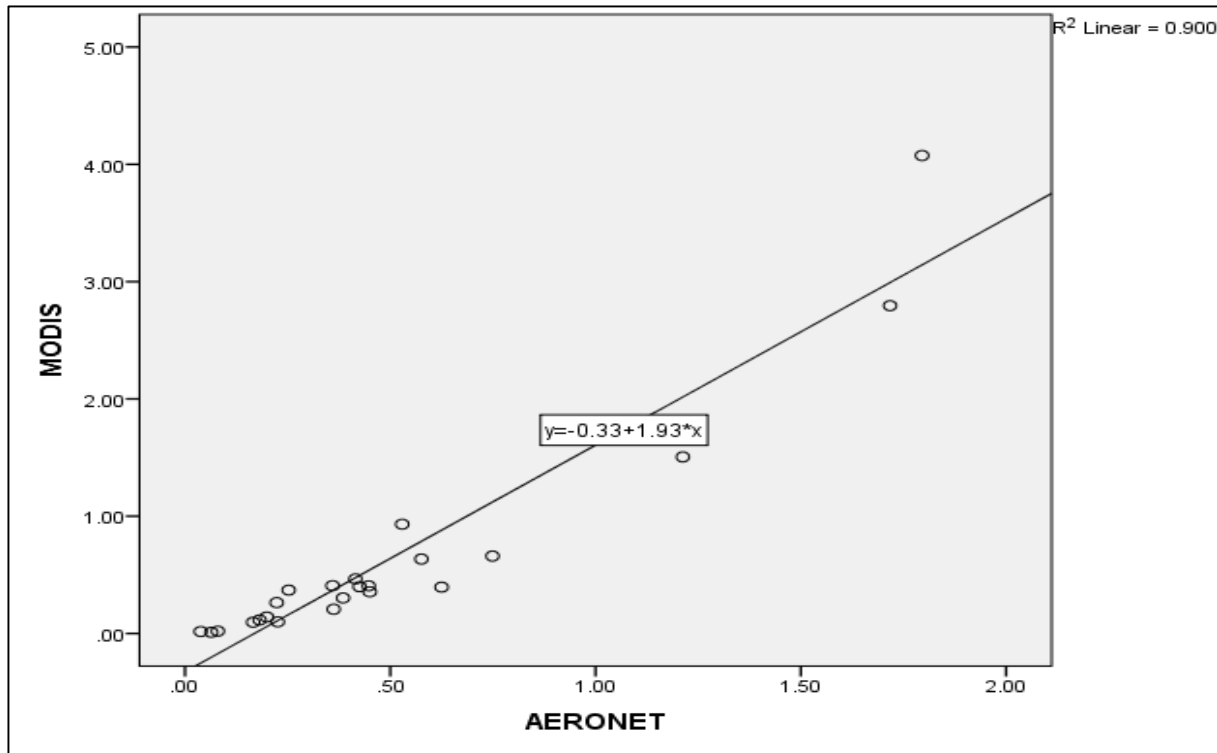


Figure 5,2: Linear Regression for Aerosol Optical Depth Derived from MODIS and AERONET using Minimum Distance Technique

- Based on the scatter plot, the coefficient of determination (R^2) value obtained in this result is 0.9 and it shows strong correlation between AOD derived from MODIS and AERONET.
- The regression equation derived from this model is $AOD_{MODIS} = 1.93 AOD_{AERONET} - 0.33$ where the intercept value is -0.33 with a slope at 1.93.

5.2 Multiple Plane Regression Technique

- Based on the tabulated table, five values of latitude and longitude for each day were chosen based on two different methods which are mean and standard deviation and relative percentage error.
- **Mean and standard deviation** The corresponding latitude and longitude for these pixels was prepared and the mean (μ) and standard deviation (σ) have been calculated by using Eq. 1 and Eq. 2.

$$\text{Mean } (\mu) = \frac{1}{n} \sum_{i=1}^n x_i \quad (1)$$

$$\text{Standard deviation } (\sigma) = \sqrt{\frac{1}{n-1} \sum_{i=1}^n (x_i - \mu)^2} \quad (2)$$

- **Relative percentage error** The corresponding latitude and longitude for these pixels was prepared and relative percentage error was calculated by using Eq. 3.

$$\text{Relative error (\%)} = \frac{\text{Predicted} - \text{Actual}}{\text{Actual}} \times 100 \quad (3)$$

- Next, the selected five point values were plotted by using scatter plot with independent variables, latitude and longitude, on the X and Y axes and dependent variable, AOD, on the Z axis for the multiple regression plane technique. These points have been fitted in the form of Eq. 4.

$$Z = aX + bY + c \quad (4)$$

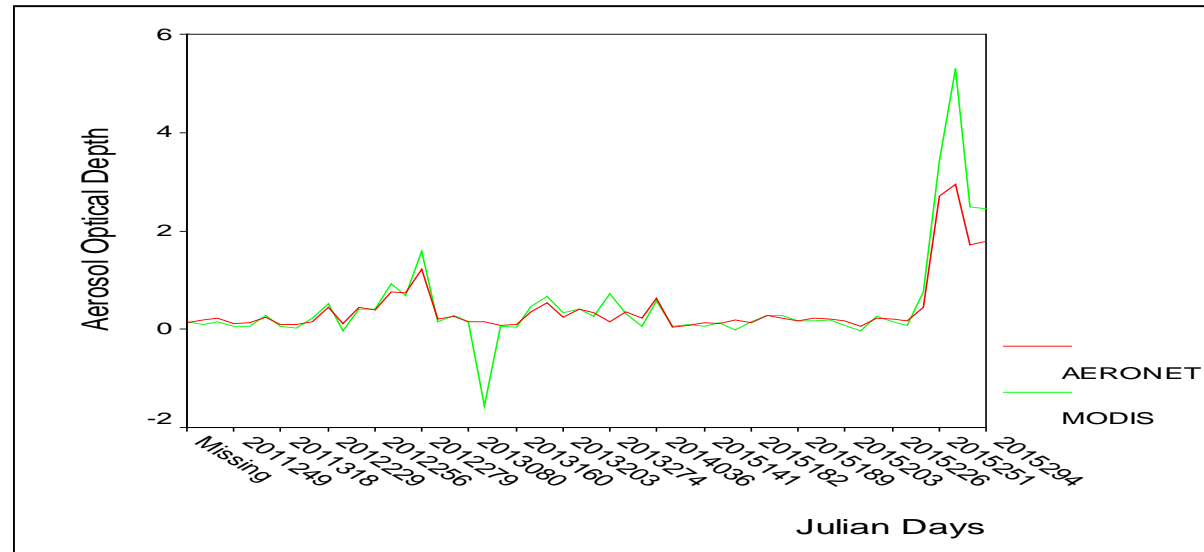


Figure 5.3: Variations of Aerosol Optical Depth for MODIS and AERONET Data using Mean and standard deviation ($\mu \pm \sigma$)

- The range value for AOD_{MODIS} is -1.56 to 5.3 while for $AOD_{AERONET}$ the minimum and maximum values were 0.04 and 2.95, respectively.
- Study by Abd Jalal, Asmat, & Ahmad, (2012) classified that In Kuching area dominant aerosols occurred in Kuching area urban and continental aerosols. Overestimation of AOD_{MODIS} occurred at Julian Day 253 in 2015 when there were extremely high of AOD_{MODIS} was observed with 5.3 while for $AOD_{AERONET}$ is only 2.9.
- There was a large underestimation for AOD_{MODIS} at Julian Day 245 in 2011 where predicted AOD_{MODIS} is -1.6 as compared with the actual value from $AOD_{AERONET}$ which only at 0.15.

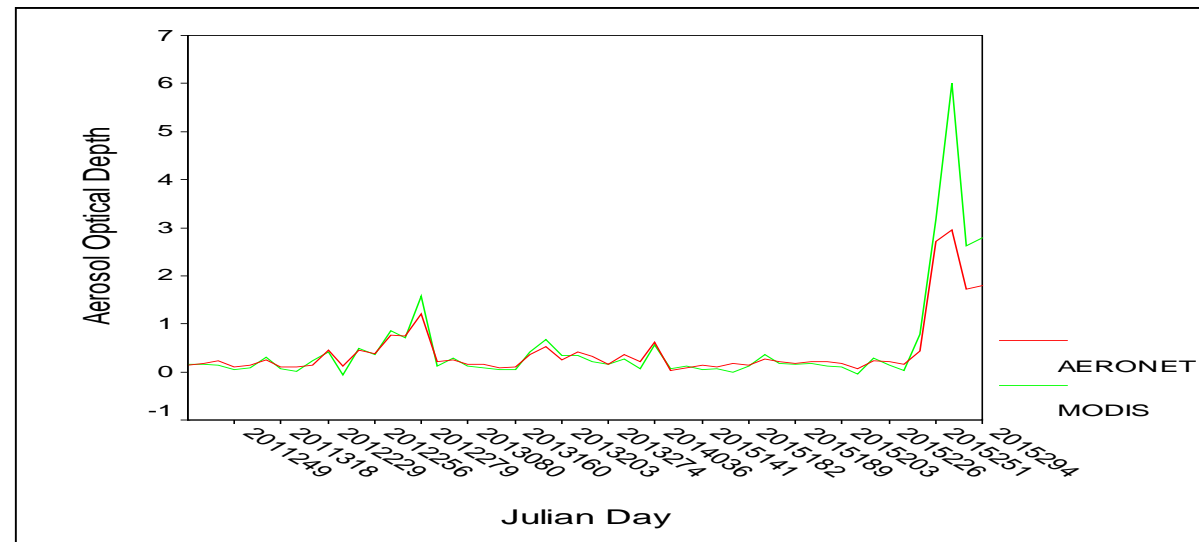
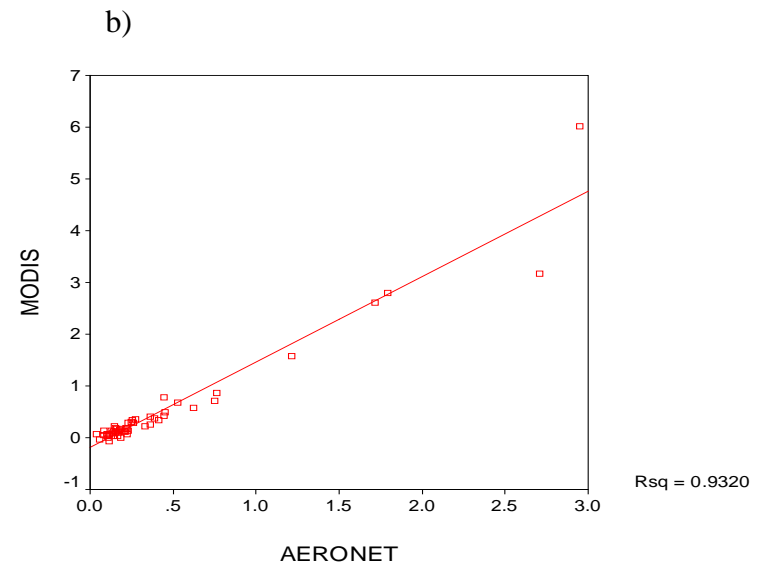
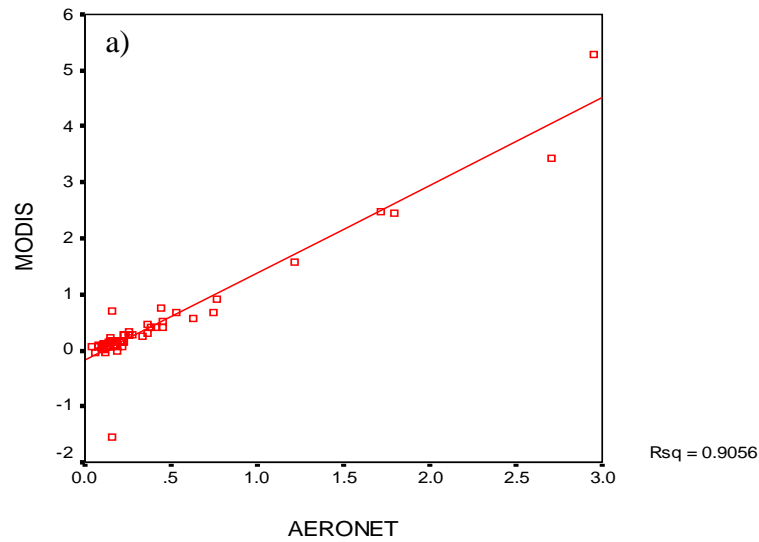


Figure 5.4: Variations of Aerosol Optical Depth for MODIS and AERONET Data using Relative Absolute Error (RAE)

- The range value for AOD_{MODIS} is -0.06 to 6.0 while for $AOD_{AERONET}$ the minimum and maximum values were 0.04 and 2.95, respectively. Overestimation of AOD_{MODIS} occurred at Julian Day 253 in 2015 when there was extremely high value of AOD_{MODIS} was observed with 6.0 and only 2.9 for $AOD_{AERONET}$.
- The distribution patterns of AOD at Kuching is basically constant where high concentration of AOD was observed during dry seasons (June to September). On the contrary, during wet seasons from November to March, the aerosol loading was monitored at low AOD.
- Same results were obtained by Salinas, Chew, Mohamad, Mahmud, & Liew, (2013) at Kuching area but data available only for 2011 where low aerosol loading basically most of the period except for the months of August and September examined high AOD values likely from regional episodes of biomass burning and fire activity during that particular months.



- The regression equation derived from this model for $\text{MODIS}_{\mu\pm\sigma}$ is $\text{MODIS}_{\text{AOD}} = 1.5609 \text{AERONET}_{\text{AOD}} - 0.1762$ and the regression equation derived from $\text{MODIS}_{\text{RAE}}$ is $\text{MODIS}_{\text{AOD}} = 1.6469 \text{AERONET}_{\text{AOD}} - 0.1811$.
- The R^2 obtained for $\text{MODIS}_{\mu\pm\sigma}$ is 0.9056 and using $\text{MODIS}_{\text{RAE}}$ is at 0.932 shows strong relationship between $\text{AOD}_{\text{MODIS}}$ and $\text{AOD}_{\text{AERONET}}$.
- For $\text{MODIS}_{\mu\pm\sigma}$, the MAPE was found to be 24% and RMSE value is 0.45 while for $\text{MODIS}_{\text{RAE}}$, the MAPE is around 12% and for RMSE is 0.47.
- There were only little differences between RMSE for $\text{MODIS}_{\mu\pm\sigma}$ and $\text{MODIS}_{\text{RAE}}$ while for MAPE value for $\text{MODIS}_{\mu\pm\sigma}$ is quite higher with 24% as compared to $\text{MODIS}_{\text{RAE}}$ with only 12%. Based on that, it shows that the selection method by using $\text{MODIS}_{\text{RAE}}$ can also be used to retrieve true value of AOD.
- Here non-zero intercepts ($A = -0.1762$ and -0.1181) for $\text{MODIS}_{\mu\pm\sigma}$ and $\text{MODIS}_{\text{RAE}}$, respectively show that the retrieval algorithm is biased at low AOD value due association with a sensor calibration error or an improper assumption on ground surface reflectance (T. X. P. Zhao et al., 2002).
- Slope higher than unity at 1.5609 for $\text{MODIS}_{\mu\pm\sigma}$ and for $\text{MODIS}_{\text{RAE}}$ at 1.6469 indicates an overestimation of AOD by MODIS with respect to AERONET retrieval.

Figure 5.5: Linear Regression for Aerosol Optical Depth from MODIS and AERONET Data a) Mean and standard deviation ($\mu\pm\sigma$) and b) Relative Absolute Error (RAE)

5.3 Artificial Neural Network (ANN)

- In this study, the artificial neural network (ANN) had been performed in constructing a model based on MODIS and AERONET as an input also AERONET AOD data as an output in this model.
- First model is by using the latitude, longitude and AOD_{MODIS} as an input and secondly, the inputs used are latitude, longitude, AOD_{MODIS} and solar zenith angle. Different input variables were tested in developing good prediction for the ANN model.
- Therefore, the objective of this analysis is to improve the results from the AOD_{MODIS} from the multiple regression plane technique to obtain AOD_{MODIS} as close as possible to the one obtained from $AOD_{AERONET}$

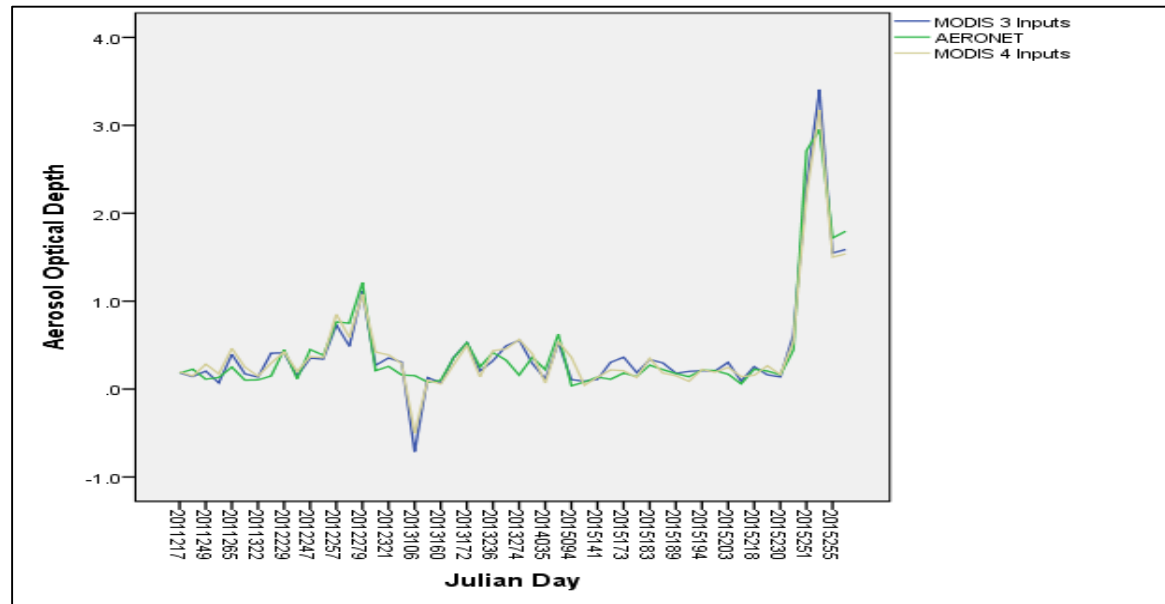
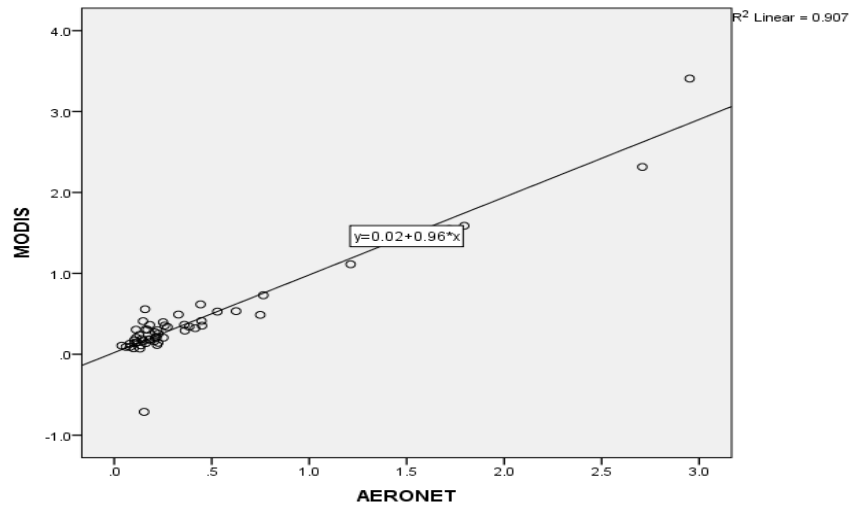
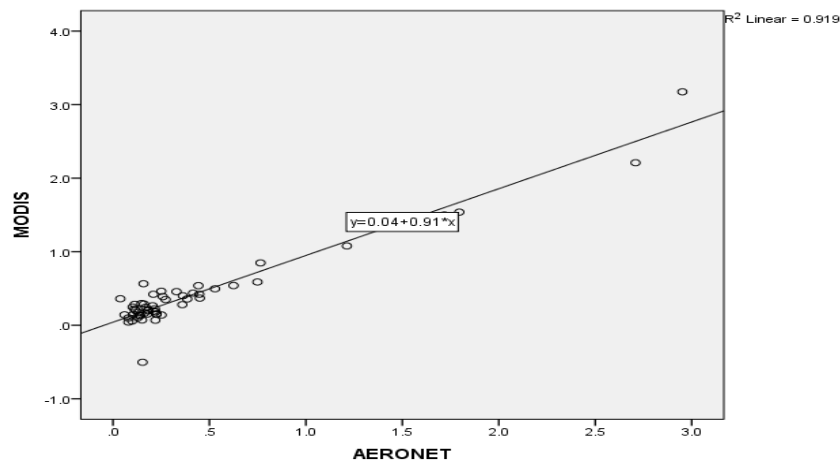


Figure 5.6: Temporal series of Aerosol Optical Depth for the direct and the improved values with the chosen method

- The variations of direct and improved AOD_{MODIS} was plotted in Figure 5.6 for both models for easy comparison.
- It shows that the improved AOD value by using Model II have the great relationship with the AERONET data.
- As explained earlier, the high variations of AOD at Julian Days may cause from the urbanization and haze episodes. There are obviously the MODIS data had underestimate and overestimate the AOD value.



b)



- The regression equation derived from this model using Model I is $MODIS_{AOD} = 0.96_{AERONET AOD} + 0.02$ and the regression equation derived from Model II is $MODIS_{AOD} = 0.91_{AERONET AOD} - 0.04$.

- The R^2 obtained for Model I is 0.907 with RMSE 0.184 and using Model II is at 0.919 and RMSE value is 0.169 shows strong relationship between improved AOD_{MODIS} and $AOD_{AERONET}$.

Figure 5.7: Linear Regression for Aerosol Optical Depth from MODIS and AERONET using a) Model I and b) Model II

5.4 Discussions

- By using minimum distance technique only several data were obtained even though the AOD value retrieved was as close as possible to the AERONET station.
- For multiple regression plane technique, the common usage for the selection of latitude and longitude for each pixel's data is based on their mean and standard deviation ($\mu \pm \sigma$). In this study, new method has been introduced by using the selection based on relative absolute error (RAE) for both latitude and longitude data and these methods are compared.
- Even though the RMSE for $\text{MODIS}_{\mu \pm \sigma}$ is quite lower than $\text{MODIS}_{\text{RAE}}$ with 0.45 and 0.47 respectively but need to compare with others statistical parameters. It shows that the MAPE for $\text{MODIS}_{\mu \pm \sigma}$ is quite high with 24% as compared to $\text{MODIS}_{\text{RAE}}$ with only 12%. Based on that, it shows that the selection method using $\text{MODIS}_{\text{RAE}}$ can also being used to retrieve better value of AOD.

5.4 Discussions

- For the improvement of AOD_{MODIS} using ANN models it shows that by using Model II consists of 4 inputs including latitude, longitude, AOD_{MODIS} and solar zenith angle may improve the AOD_{MODIS} values.
- Thus, from the comparison shows the importance of modifying the existing technique for the retrieval of AOD to reduce the error and uncertainties during the application of the parameter into radiative transfer model.
- Therefore, it is required to improve the MODIS retrieval algorithm because radiative transfer simulations should be bearing in mind that they have an uncertainty generated by uncertainties in the outputs.
- The limitation of this study was low availability for AOD value derived from MODIS. As the conclusion, the requirement for another satellite data is necessary so that it can provide more information for further analysis.

Way forward

- To strengthen the aerosol studies as an established aerosol community in Malaysia under Clean Air Society Forum of Malaysia (Dr Noor Zaitun Yahaya)
- To proposed Ultrafine Particles (mass/particle number) South East Asia (SEA) Network (UFP-SEANET)
- To explore vertical measurement of particles at urban and high altitude areas in selected region in Malaysia and SEA